

CR-184169

Richard Co. go  
EH33

**FINAL REPORT**

**Contract NAS8-37195**

**CHEMICAL WASTE DISPOSAL IN SPACE BY PLASMA DISCHARGE**

**BY**

**Professor James K. Baird**

**Prepared for**

**National Aeronautics and Space Administration  
George C. Marshall Space Flight Center  
Marshall Space Flight Center**

**Submitted by**

**The University of Alabama in Huntsville  
College of Science  
Huntsville, Alabama 35899**

**March 31, 1991**

(NASA-CR-184169) CHEMICAL WASTE DISPOSAL IN  
SPACE BY PLASMA DISCHARGE Final Report  
(Alabama Univ.) 68 p CSCL 06K

N91-29737

Unclas  
63/54 0038006

1. Introduction.....	3
1.1 Radiation Chemistry.....	4
1.2 Plasma Chemistry.....	4
2. Experimental Considerations.....	6
2.1 Absorbed power.....	6
2.2 Identification of Intermediates and End-Products.....	7
2.3 G-value for Plasma Decomposition.....	7
3. Instrumentation.....	8
Table 1. Equipment Specifications.....	9
Figure 1. A Schematic of the Experimental Layout.....	10
Results.....	11
Ammonia.....	11
Experimental Results.....	11
Discussion.....	12
Diagrams.....	15
Figures 2 - 23. G(-NH <sub>3</sub> ) and Beta versus Power.....	15
Figures 22 - 33. G(-NH <sub>3</sub> ) and Beta versus Flowrate.....	36
Figures 34 - 46. G(-NH <sub>3</sub> ) and Beta versus Pressure.....	48
Nitrous Oxide.....	62
Methane.....	62
Conclusions.....	63
References.....	64
Appendix A.....	67

### Abstract.

We have constructed an inductively coupled plasma discharge apparatus operating at 13.56 MHz and with electrical power up to 2.5 kW. We have tested the efficiency of this device to destroy various gases expected to be carried aboard the Space Station. By expressing the efficiency of our device in terms of the G-value (which is the number of molecules decomposed per 100 eV of energy absorbed), we have been able to compare our results with the known efficiencies of ionizing radiation to destroy these same gases.

In the case of ammonia, which we studied extensively, we found that in our inductively coupled device, the destruction efficiency,  $G(-\text{NH}_3)$  varied from 6.0 to 32.0 molecules/100 eV, depending upon conditions. The reciprocal of the G-value is the specific energy efficiency. Expressed in engineering units, our measured  $G(-\text{NH}_3)$  values correspond to a range of specific energy efficiencies lying between 0.45 and 0.084 kWhr/mole. These figures put our inductively coupled plasma method well within the electrical generating capabilities available on spacecraft.

By comparison, we found that capacitatively coupled discharges were less efficient in destroying ammonia than our inductively coupled discharge. For capacitive coupling, the value of  $G(-\text{NH}_3)$  lies in the range 6 - 20 molecules/100 eV, depending upon conditions.

In the case of ammonia destruction, we found that the  $G(-\text{NH}_3)$  was a qualitative guide to the efficiencies of plasmas. The value of  $G(-\text{NH}_3)$  is independent of whether the ionizing radiation is alpha, beta, or gamma, which indicates that secondary electrons are responsible for the chemical change. Depending upon conditions,  $G(-\text{NH}_3)$  in the case of ionizing radiation lies within the range 2.7 - 10 molecules/100 eV.

Our plasma device was also used to destroy nitrous oxide and methane. We found  $G(-\text{N}_2\text{O})$  to lie in the range 3.0 - 8.8 molecules/100 eV depending upon conditions. No quantitative data was obtained with methane, although it was noticed that the discharge converted the gas into a yellowish-brown polymer.

Finally, we have shown how the G-value for the destruction of any gas can be computed theoretically from a knowledge of the electron velocity distribution, the various electron-molecule scattering cross sections, and the rate constants for the reactions of secondary species produced by the discharge. Since the radiation and plasma chemistries of a given gas are thought to be dominated by the electron-molecule collisions, our theory is the first step toward unifying these two areas.

## 1. Introduction.

To utilize a plasma discharge as a means to decompose chemical by-products into their constituents, basic information on the chemical and physical processes that govern the plasma's behavior is required. Inductively-coupled r.f. plasma chemical reactors offer high enthalpy and an environment free of any electron contamination; however, to obtain an understanding of the elementary processes that occur in even the simplest plasma system is an extremely complex task. In most instances, a complete picture of the chemical processes occurring in a r.f. plasma reactor would require analyses of r.f. heating, heat transfer, fluid mechanics, nucleation and particle growth, chemical kinetics, and the state of thermodynamic equilibrium.

To circumvent the relative lack of experimental data available, attempts have been made to model r.f. plasmas, but these have concentrated mainly on chemically inert systems [1-12]. For example, Zhao *et.al.* have developed a model taking kinetic effects into account [8, 9]. The scope of the problem, however, reduced the testing of the model to relatively simple systems. In a series of papers [1, 2], Chang and Pfender developed a two temperature model for argon plasmas in chemical (ionization) non-equilibrium. They concluded that the assumption of local thermal equilibrium (LTE) was not valid for low pressure plasma jets and that previous modeling attempts based on this assumption were inadequate. This conclusion is also supported by a number of experimental studies [13-19], which have concentrated mainly on the macroscopic properties of the plasma, such as end-product distribution [19], pressure distributions [17] and flowrate [15, 16, 19] as opposed to the kinetic properties, such as electron temperature and density. When temperature measurements have been made, however, the lack of agreement on operating conditions such as pressure, flowrate and input power has often hampered comparison of results [14-18].

In this report we have investigated whether a possible solution to this lack of available data could be found in the possible similarity between the chemical processes that

occur in plasma chemistry and in radiation chemistry. It follows that if links can be forged between these two areas of research, the extensive radiation chemical literature could be exploited to assist in interpreting the chemical processes that occur in low temperature plasmas.

### **1.1 Radiation Chemistry.**

In radiation chemistry, the radiation dose is defined as the amount of energy absorbed per unit mass and the equivalent of the quantum yield, the G-value, is the number of molecules reacted per 100 eV of ionizing radiation absorbed. The G-value serves to express the energy efficiency of the reaction. Although G often depends upon pressure, temperature, and gas flowrate, it is in general independent of linear energy transfer (L.E.T.); that is to say, it is independent of the whether the type of incident radiation is alpha, beta, or gamma.

The energy required to create an electron-ion pair due to the action of ionizing radiation is called W; having a value of about 30 eV. W depends weakly on the chemical nature of the gas; for example, at 30 eV per energy loss event, a 4.5 MeV alpha particle creates about 150,000 electron-ion pairs before coming to rest in a gas. Through inelastic electron-molecule collisions, the electrons, in turn, transfer their energy to the gas. Under conditions of continuous irradiation, a steady state distribution of electron velocities is established. To the extent that G is independent of L.E.T., the electrons dominate the radiolysis of the gas.

### **1.2 Plasma Chemistry.**

In plasma chemistry, energy is coupled into a gas from an external source, such as in this case, a radio-frequency generator. Between collisions with atoms or molecules, the electrons in the plasma gain energy from the r.f. field until a steady state is achieved. In a low pressure discharge, most of the chemical change is initiated by inelastic electron-molecule impacts. As in radiation chemistry, these collisions create primary species which proceed through a sequence of secondary reactions to produce the products. Burton and

Funabashi have noted this similarity between radiation and plasma chemistry, but have pointed out also that the distributions of electron velocities prevailing in the gas in the two cases are likely to be different [22].

Although ubiquitous in radiation chemistry, the G-value concept has been used only sparingly in plasma chemistry. On the occasion when it appears, it is usually expressed in terms of macroscopic units, such as kg/kW hr or mol/kW hr. Only the latter is independent of molecular weight and therefore convertible to G (molecules/100 eV) through the equation  $G(\text{molecules}/100 \text{ eV}) = 2.68G(\text{mol}/\text{kW h})$ . When so converted, the values reported in the plasma literature often lie in the same range with respect to order of magnitude as typical radiolysis values. In glow discharges, Burton found for the disappearance of methane,  $G(-\text{CH}_4) = 20 \text{ molecules}/100 \text{ eV}$  [23] (in radiolysis,  $G(-\text{CH}_4) = 7.5 \text{ molecules}/100 \text{ eV}$  [24]), and for the disappearance of butane,  $G(-\text{C}_4\text{H}_{10}) = 16 \text{ molecules}/100 \text{ eV}$  [25] (in radiolysis,  $G(-\text{C}_4\text{H}_{10}) = 10 \text{ molecules}/100 \text{ eV}$  [26]), where the minus sign denotes consumption of the molecule concerned. Fauchais and Rakowitz [27] reported in passing that in a d.c. plasma jet containing  $\text{N}_2$  and  $\text{O}_2$ , NO was produced with a yield which converted to  $G(\text{NO}) = 3.6 \text{ molecules}/100 \text{ eV}$ . Bell [28], analyzing the data of Mearns and Morris [29] on the production of atomic oxygen from  $\text{O}_2$  in a microwave plasma, found that although  $G(\text{O})$  depended upon operating conditions, its value lay always within the general range of 1.5 - 12.5 atoms/100 eV.

In a recent paper published with support from this contract [30] (for a reprint, see the Appendix A), we have derived a formula for the G-value for a general plasma chemical reaction involving a gas, A, in terms of macroscopic parameters describing the plasma

$$G(-A) = \frac{7.17\beta\Phi_{\text{STD}}}{W} \quad 1)$$

In order to compare the radiolysis and plasma G-values for a given gas, it is useful to calculate the plasma equivalent of dose. For ammonia, the dose in eV/g is given by

$$D = 4.93 \times 10^{23} \frac{W}{\Phi_{STD}} \quad 2)$$

where  $\beta$  is the fraction of A that is transformed,  $\Phi_{STD}$  is the flowrate in standard liters per minute and W is the total power (kW) absorbed by the plasma.

Applying this equation to data reported by d'Agostino *et.al.* on the capacitatively coupled plasma decomposition of ammonia [19], we found that G(-NH<sub>3</sub>) depended on operating conditions but lay in the range of 6 - 20 molecules/100 eV. In this experimental study, the dependence of G(-NH<sub>3</sub>), for an inductively coupled plasma, on the various operating parameters is investigated. These results are then compared with those reported by Peterson [32] for the gas phase radiolysis of ammonia (where G(-NH<sub>3</sub>) lay in the range of 2.7 - 10 molecules/100 eV). The possibility that similarities with respect to magnitude might be due to some common features of the reaction mechanism is then discussed.

## 2. Experimental Considerations.

To characterize fully the overall chemical reaction associated with any plasma process it is necessary to know not only the dependence of product yields on operating conditions but also the reaction mechanism giving rise to those end-products. However, to compare the results from plasma chemistry with those of radiation chemistry only the basic experimental parameters needed to characterize the system. These are, absorbed power, gas mixture, gas flowrate, pressure, fraction of gas decomposed  $\beta$ , end-product distribution and in our case, the G-value, which is derivable from the former through Eq.(1). Of these parameters, input gas mixture, flowrate, and pressure are independent variables. In the work encompassed by this report, we have confined our experiments to flowrates of 0 - 3 l/min (STD) and pressures of 3.5 - 40 Torr. The remaining parameters are dependent variables, and we shall discuss each in turn.

### 2.1 Absorbed power.

One of the most important parameters needed to characterize a plasma chemical process is the amount of energy that has been absorbed by the gas. The plasma was heated

inductively using a 2.5 kW, 13.56 MHz r.f. generator coupled via an impedance matching unit to a 4 -5 turn work coil. By surrounding the plasma vessel with an insulated water jacket and correcting the observed temperature rise for the endothermicity or exothermicity of the overall plasma reaction, we determined the power absorbed.

## **2.2 Identification of Intermediates and End-Products.**

The composition of the intermediates and the end-products produced by the discharge provides information on the chemical pathways operating in the plasma. This information is, incidentally, crucial in many other applications, such as plasma etching, the conversion of methane to acetylene, and the purity of a-C:H deposits. The diagnostic methods available include residual pressure measurements (effective in the case of ammonia, since the products  $N_2$  and  $H_2$  are non-condensable)[31, 36, 37], and mass spectroscopy [19, 39-44].

In general, the distribution of products is a function of the power absorbed, flowrate, and pressure. In some cases, there has been a lack of agreement between different studies in regard to intermediates and end products. A case in point is ammonia, wherein  $N_2H_4$  has been found to be a major product in some systems [45] and yet not detectable at all in others [19, 31, 46].

## **2.3 G-value for Plasma Decomposition.**

The experimental parameters required to determine the G-value are the power absorbed, the conversion fraction of the reactant or product, and the overall flowrate. These parameters have all been determined or are available, therefore  $G(-NH_3)$  can be calculated from Equation 1.

With the determination of the plasma G-values, a comparison with radiation G-values will be undertaken to evaluate the possible contribution radiation chemistry may play in establishing the dominant excitation mechanisms existing in low temperature plasmas.

### 3. Instrumentation.

A schematic diagram of the apparatus is given in Figure 1 and the equipment specifications are given in Table 1. The r.f. power is supplied by a 2.5 kW RF Plasma Products Inc., Model HFS2500-D generator at a fixed frequency of 13.56 MHz. The r.f. power is fed via a coaxial cable, RG 217/U, to a RF Plasma Products Inc., Model AMN 2501E, impedance matching unit which matches the 50 ohm output impedance of the generator to the four-turn copper work-coil used to couple the power into the plasma. The input and reflected power are monitored by an in-line r.f. power watt-meter. The matching of the plasma impedance to that of the r.f. generator was achieved by the manual tuning of the impedance matching unit so as to achieve the lowest possible reflected power level. It was generally possible to maintain the reflected power below 10 Watts.

The plasma is generated and maintained in a 1 meter fused quartz tube, ID = 35 mm, which is encased by a water jacket, ID = 56 mm, for calorimetric measurements. Temperature changes in the water are monitored using thermocouples which permitted the evaluate of the actual power deposited into the plasma. The gas flow rate is controlled using a MKS Model 1159B 0 - 5 l/min Mass Flow Controller.

The vacuum system is pumped down using a 310 l/min Precision Vacuum Pump, Model DD310. The operating pressure is maintained in the region of 1 to 50 Torr using a valve system in conjunction with a Granville-Phillips Convectron vacuum gauge, Series 275.

The end-products are trapped using LN<sub>2</sub> traps and following re-warming are then analyzed. The analysis is achieved by the introduction of samples are into a Perkin-Elmer 8420 Capillary Gas Chromatograph via a Valco Instruments Co. Inc. Gas Sample Valve. Using a Chrompack PLOT fused Silica 25 m x 0.32 mm ID column coated with molsieve 5A the various components were separated and then identified using a Perkin-Elmer ITD ion trap mass spectrometer.

**Table 1. Equipment Specifications.**

**rf Plasma Generator:**

A RF Plasma Products Inc. supplied Model HFS2500-D generator together with the Model AMN 2501E impedance matching unit.

Operating Frequency: 13.56 MHz.  
 Input Power: 0 - 2.5 kW.  
 Reflected Power: < 25 W.

**Work Coil:**

Four-turn water-cooled copper tubing.

Tubing: 5 mm OD, 3 mm ID.  
 Radius: 32 mm.  
 Length: 28 mm.  
 Coolant: Deionized H<sub>2</sub>O recycled through a heat exchanger.

**Plasma Torch Assembly:**

Two concentric fused quartz tubes, the outer tube being the calorimetric water jacket.

Plasma tube: 45 mm OD, 42 mm ID.  
 Water Jacket: 58 mm OD, 54 mm ID.  
 Tube ends: Machined Teflon with Teflon O-rings.  
 Coolant: Deionized H<sub>2</sub>O.

**Temperature Measurements:**

Two K-type thermocouples immersed in the H<sub>2</sub>O flow connected to a Fluke digital multimeter, Model 45 via a Fluke 80TK thermocouple module.

**Gas Supply:**

Type: Ammonia, anhydrous 99.99%.  
 Measurement: 0 - 5 l/min (STP) MKS Model 1159B mass flow controller.

**Pressure: variable via adjustable valves.**

Measurement: Granville-Phillips Convectron vacuum gauge, Series 275.  
 Pump: 310 l/min Precision Vacuum Pump, Model DD310.

**End-product analysis:**

Gas samples analyzed using GC/MS.

Perkin-Elmer 8420 Capillary Gas Chromatograph.

Column: Chrompack PLOT fused Silica 25 m x 0.32 mm ID column coated with molsieve 5A.

Gas Sample Valve: Valco Instruments Co. Inc.

Mass Spectrometer: Perkin-Elmer ITD ion trap mass spectrometer.

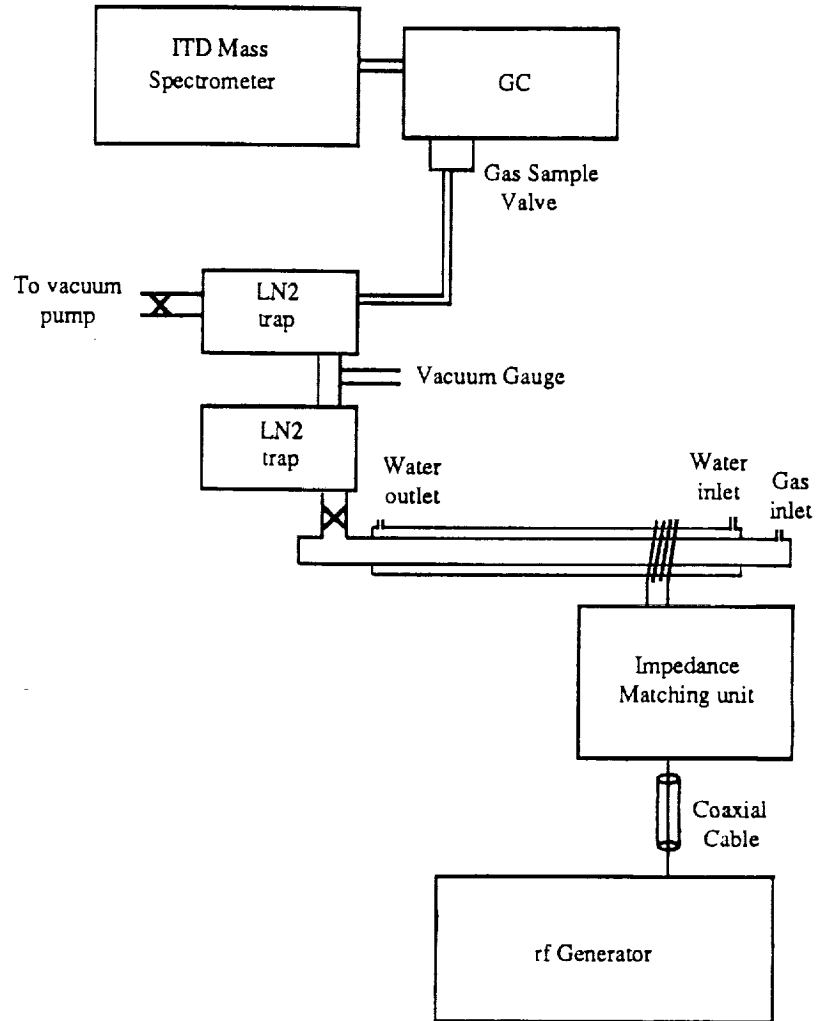


Figure 1:  
A Schematic Diagram of the Experimental Layout.

## Results.

### Ammonia.

#### Experimental Results.

A series of experiments were performed to measure the degree,  $\beta$ , of decomposition of the ammonia. From these results we calculated the G-value ( $G(-\text{NH}_3)$ ) in terms of the power deposited into the plasma (kW), the operating pressure (Torr) and the flowrate (Liters/min). It was possible to establish a steady state plasma discharge over a wide range of pressures, flowrates and input power. This plasma forms a pinkish-red doughnut shape within the work-coil. The central region of the discharge is darker in color due to lower temperature in this area. Depending on pressure, flowrate and input power the tail-flame was found to extend from the end of the work-coil out to approximately 60 cm.

Initial experiments measured the dependence of  $\beta$  on pressure, and input power at a constant flowrate. Ideally, from Equation 1, if  $\beta$  is proportional to the input power under all conditions then  $G(-\text{NH}_3)$  will be a constant. Therefore to establish the relationship existing between  $\beta$  and the plasma G-value we plotted both  $\beta$  and G on the same graph. Figures 3 - 23 give the results of these experiments. At a gas pressure of 3.5 Torr (Figs.3 & 4) it is evident that the ammonia is completely decomposed at power levels below 0.5 kW. As the pressure is increased slowly up to 30 Torr, at a constant flowrate of 1 l/min, (Figs.3-10) the power required to completely decompose the ammonia increases to approximately 1 kW. At every pressure level at this flowrate, the G-value decreases with increasing  $\beta$  and does not appear to provide a parameter independent of the input power. Overall, as the pressure increases, the maximum G-value decreases from approximately 20 down to 10.

Repeating these experiments at a flowrate of 2 l/min, similar results are obtained (see Figs.12 - 18). The maximum power required to completely decompose the ammonia increased to 1.8 kW at a pressure of 30 Torr. At 3 l/min, it proved impossible, with the

available power (up to 2.5 kW), to completely decompose the ammonia (Figs.19-23). The maximum G-value increased to 38 but overall the G-value remained dependent on the operating conditions. The rate of decomposition reached a maximum at approximately  $\beta = 0.8$  whereupon further increases in power tended to decrease the yield slightly. This result suggests a possible synthesis mechanism of ammonia may be occurring. We attempted to synthesis ammonia by plasma discharge using  $H_2$  and  $N_2$  under a wide range of operating conditions but were unable to produce more than approximately 1%  $NH_3$ . However, in the case of an ammonia plasma the possible presence of a variety of radicals and other possible intermediates may provide a more efficient pathway to synthesis  $NH_3$ .

Figures 24-35 give the relationship of  $\beta$  and the plasma G-value with respect to the gas flowrate at fixed power and pressure levels. These graphs demonstrate that  $\beta$  and  $G(-NH_3)$  are inversely related to each other for the range of flowrates considered.

A comparison of the relationship that the plasma pressure has on the decomposition of ammonia is given in Figs.36-48. These graphs clearly demonstrate that  $G(-NH_3)$ , rather than remaining constant, is directly proportional to the degree of decomposition of ammonia,  $\beta$ .

### Discussion.

In his review of the radiation chemistry of ammonia, Peterson [32] noted that in numerous ammonia gas-phase radiolysis experiments the only products detected were  $H_2$ ,  $N_2$  and  $N_2H_4$ .

In general, the product yields reported depended upon pressure, temperature, flowrate and dose rate. The values of  $G(-NH_3)$  obtained by the various authors at 20 °C, 1 atm pressure and zero flowrate lie in the range 2.7-10 molecules/100 eV and are independent of the linear energy transfer (LET) of the ionizing radiation. The total absorbed dose in every case was sufficiently low that saturation of  $G(-NH_3)$  due to high conversion was not observed. Up to dose rates of  $2 \times 10^{18}$  eV/gs, the only detectable products were  $H_2$  and  $N_2$ ; moreover, the yields of  $H_2$  and  $N_2$  were independent of dose up to  $8 \times 10^{22}$

eV/g.  $G(-\text{NH}_3)$  varied strongly with temperature, however, starting at approximately 3 molecules/100 eV at 20 °C and rising to 10 molecules/100 eV at temperatures above 225 °C. By comparison, the limited data on the photodestruction of  $\text{NH}_3$  also indicate a trend toward increasing quantum yield over the same temperature range. At dose rates in excess of  $10^{26}$  eV/gs, hydrazine was reported just detectable in the radiolyses. In flowing systems, by comparison, hydrazine was obtained with a yield of 3.95 molecules/100 eV at dose rates of  $10^{26}$  eV/gs from ammonia moving at 2.4 liters/min.

In the case of the plasma experiments undertaken here the electrical equivalent dose rates lie in the general regime  $3 \times 10^{22}$  -  $1.2 \times 10^{24}$  eV/gs. By comparison with the radiolysis experiments, these rates are intermediate between the lowest ( $3 \times 10^{15}$  eV/gs, achieved in steady-state) and the highest ( $2 \times 10^{27}$  eV/gs, achieved only in pulse radiolysis) reported by Peterson but are close to the levels used by d'Agostino *et al.* These dose levels fail by some orders of magnitude to reach the threshold of  $10^{26}$  eV/gs, where hydrazine appears under both static and flowing conditions. The lack of hydrazine in both our and d'Agostino's studies raises questions regarding the hydrazine production. In ref.[30] we proposed the possibility that, at the high-power density achieved in radiolysis, the population density of  $\text{NH}_2$  radicals is sufficient to form  $\text{N}_2\text{H}_4$  in competition with the formation of  $\text{H}_2$ . To answer this question completely requires a spectroscopic study to determine the actual population distribution that exists in the plasma.

The complete decomposition of ammonia has been shown in the case of static radiolysis experiments at 1 atm and 20 °C to require a dose exceeding  $8 \times 10^{22}$  eV/g. In the plasma experiments described in this report, we found that the electrical equivalent dose required to completely decompose the ammonia varied from  $2.2 \times 10^{23}$  to  $6.4 \times 10^{23}$  eV/g for flowrates of 1 and 2 liters/min and pressures from 3.5 to 40 Torr.

Finally, we note from our experiments that the values obtained for  $G(-\text{NH}_3)$  range from 6.0 - 32.0 molecules/100 eV, which is in reasonable agreement with that calculated from d'Agostino *et al.*'s plasma data of 6.0 - 20 molecules/100 eV. On the other

hand, in the radiolysis experiments the values for  $G(-\text{NH}_3)$  vary in the range of 2.7 - 10 molecules/100 eV. The value of 10 molecules/100 eV was achieved only at gas temperatures in excess of 225 °C. The heavy particle kinetic energy in the plasma probably lies in the range of 200 to 2000 °C, the effect of this elevated temperature may be behind the higher G-values found in the case of plasmas.

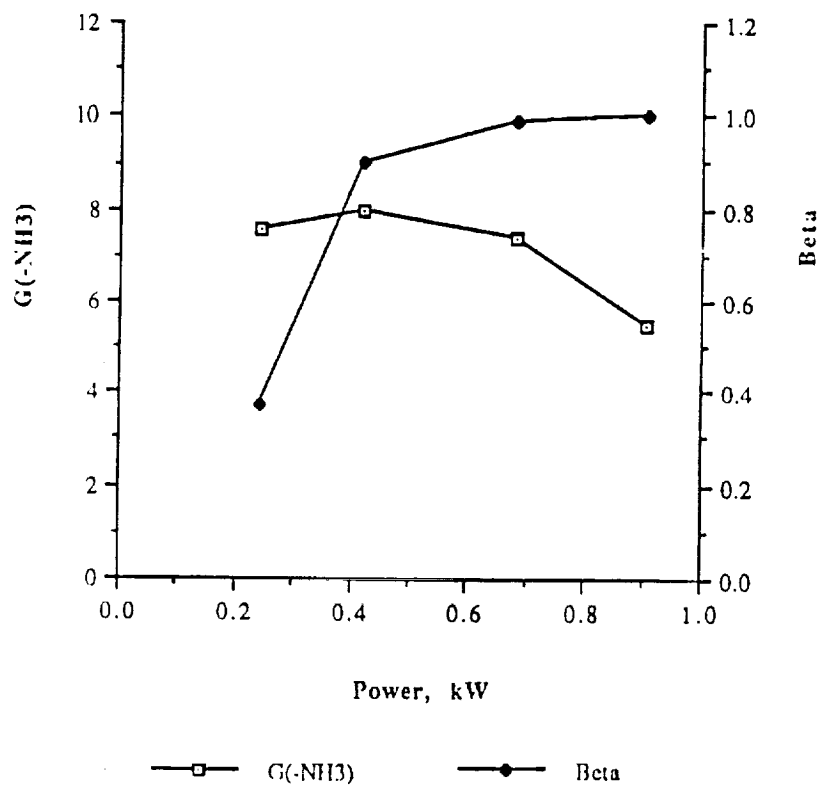


Figure 3: Dependence of the G-value and Beta of Ammonia on The Input Power. Flowrate 0.7 l/min, Pressure 3.5 Torr.

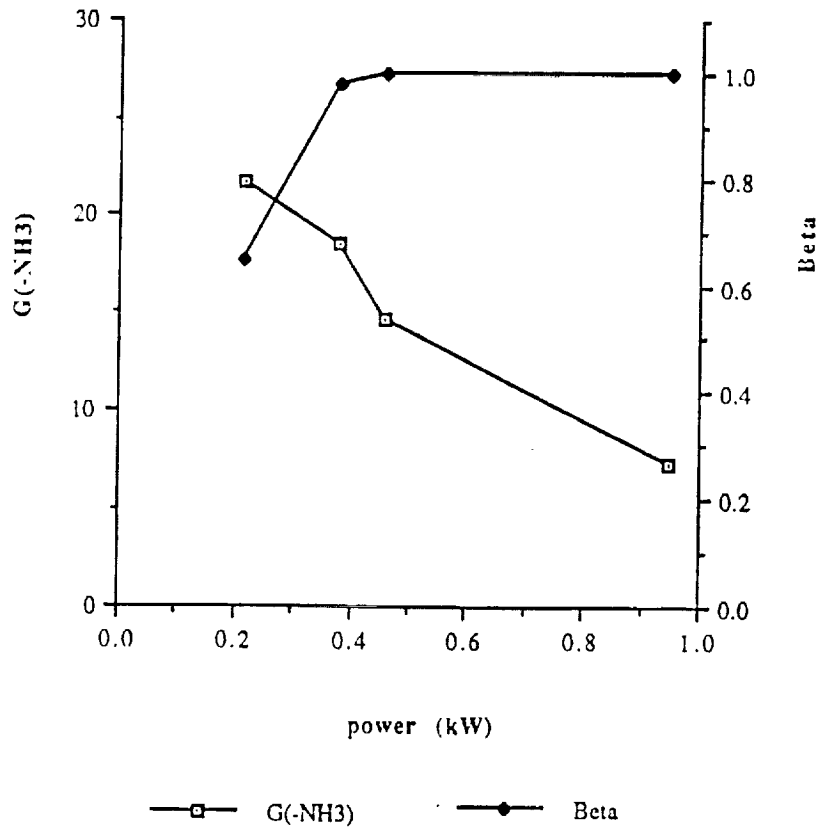


Figure 4: Ammonia, flowrate 1 l/min, pressure 3.6 Torr.

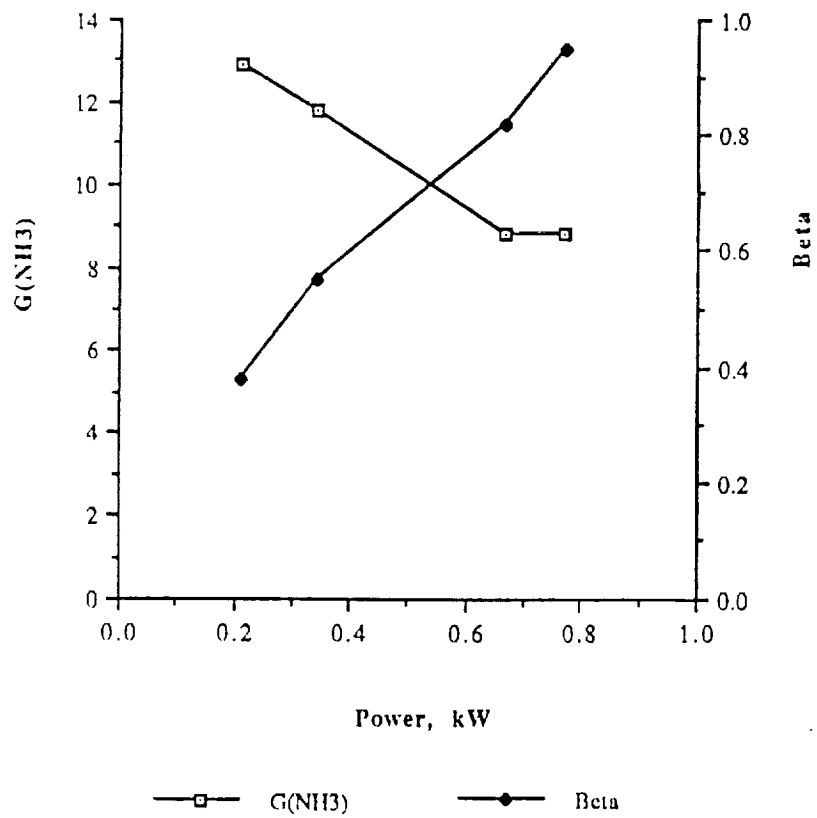


Figure 5: Ammonia, flowrate 1 l/min, Pressure 5 Torr.

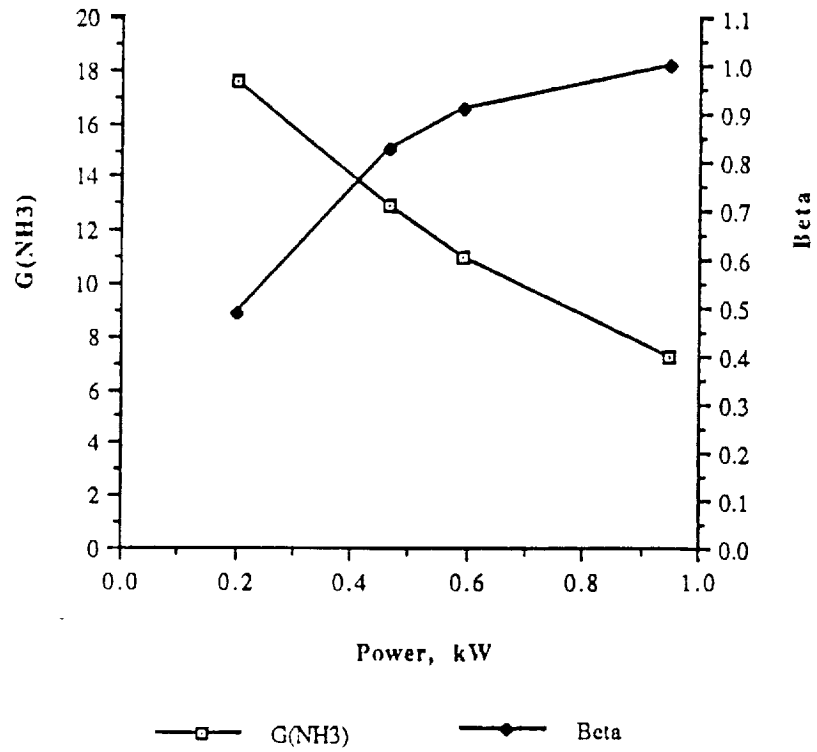


Figure 6: Ammonia, flowrate 1 l/min, Pressure 7.5 Torr.

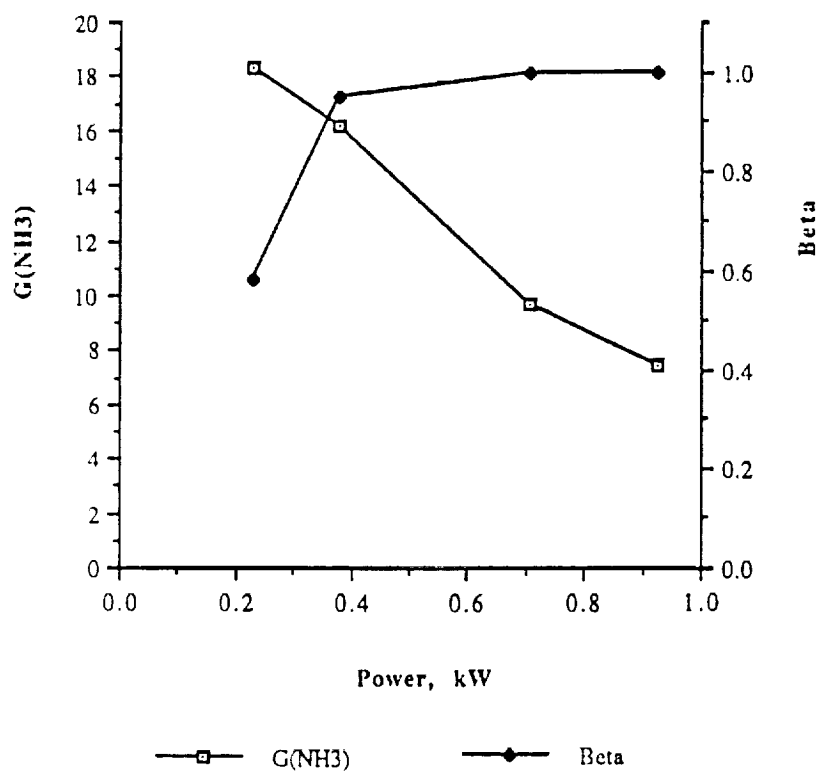


Figure 7: Ammonia, Flowrate 1 l/min, Pressure 10 Torr.

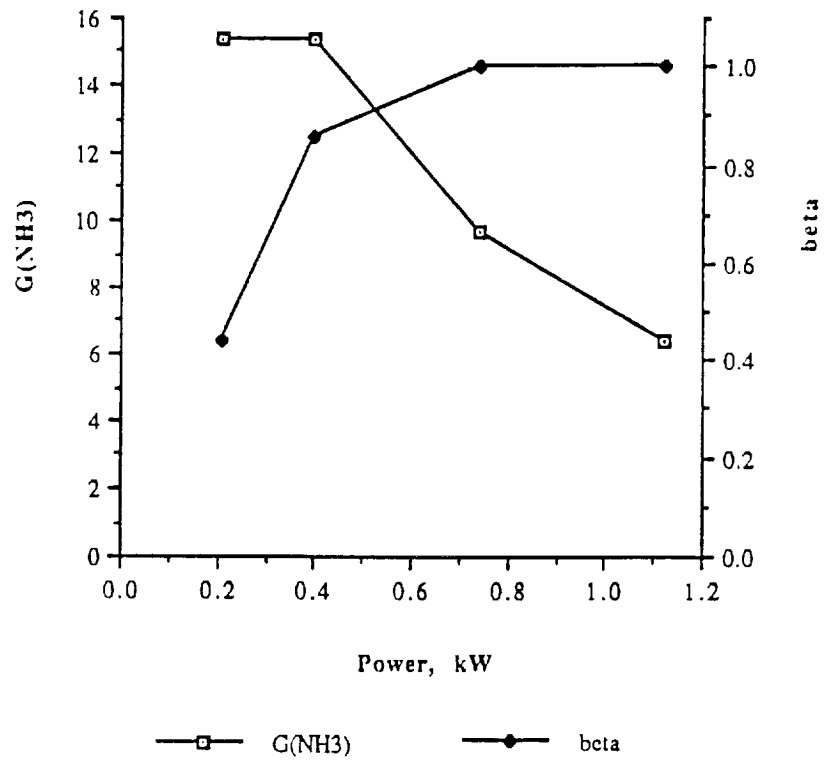


Figure 8: Ammonia, Flowrate 1 l/min, Pressure 15 Torr.

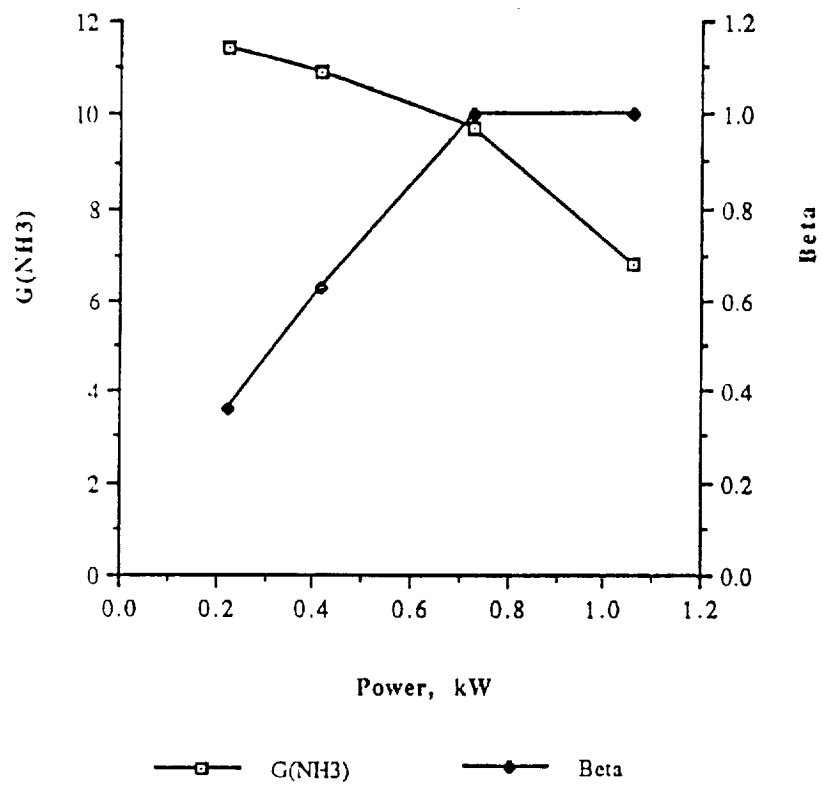


Figure 9: Ammonia, Flowrate 1 l/min, Pressure 20 Torr.

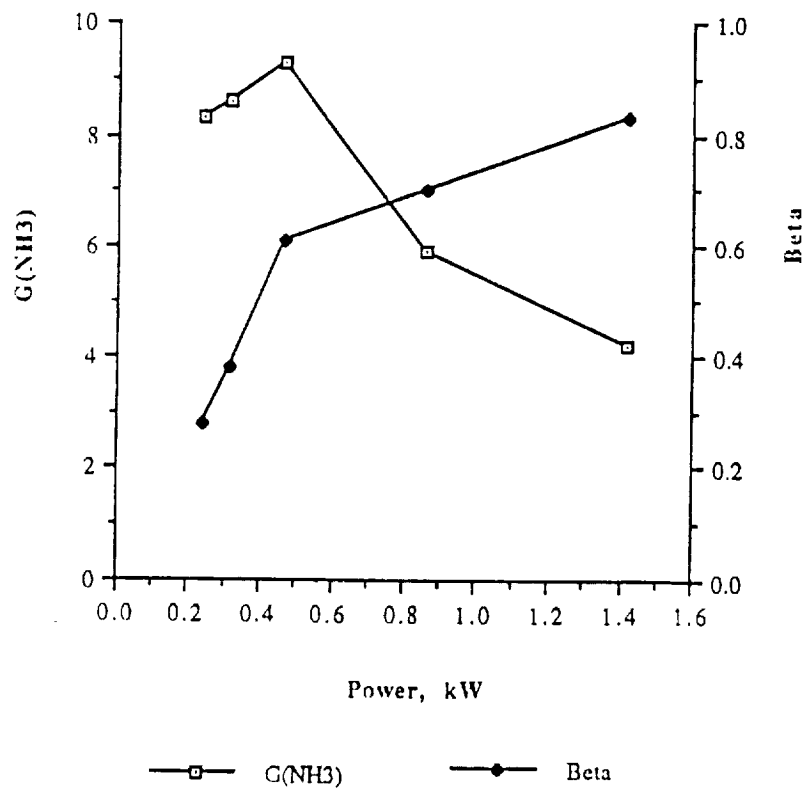


Figure 10: Ammonia, Flow-rate 1 l/min, Pressure 25 Torr.

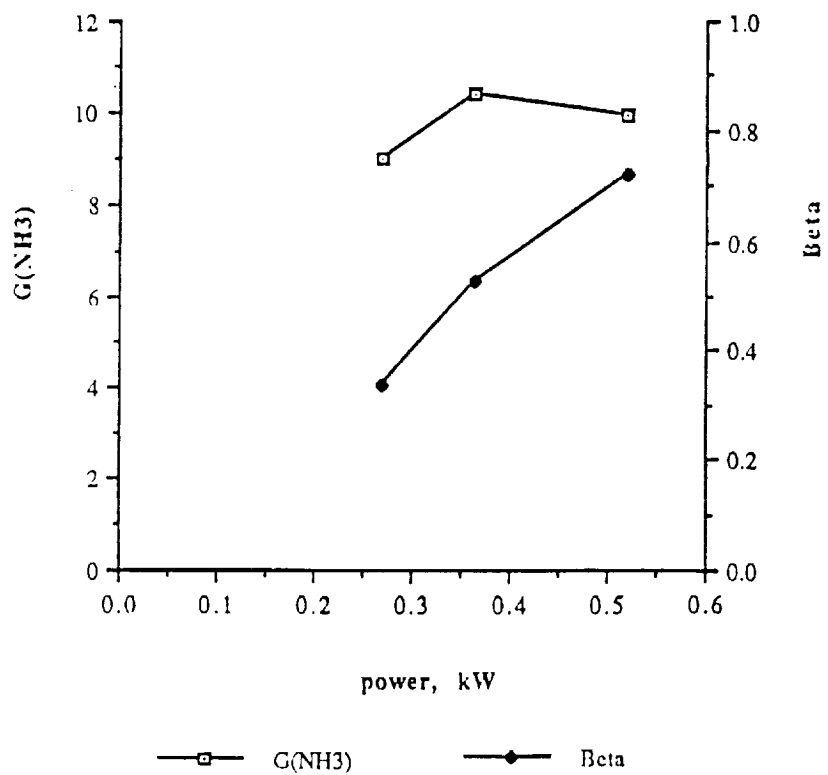


Figure 11: Ammonia, Flowrate 1 l/min, Pressure 30 Torr.

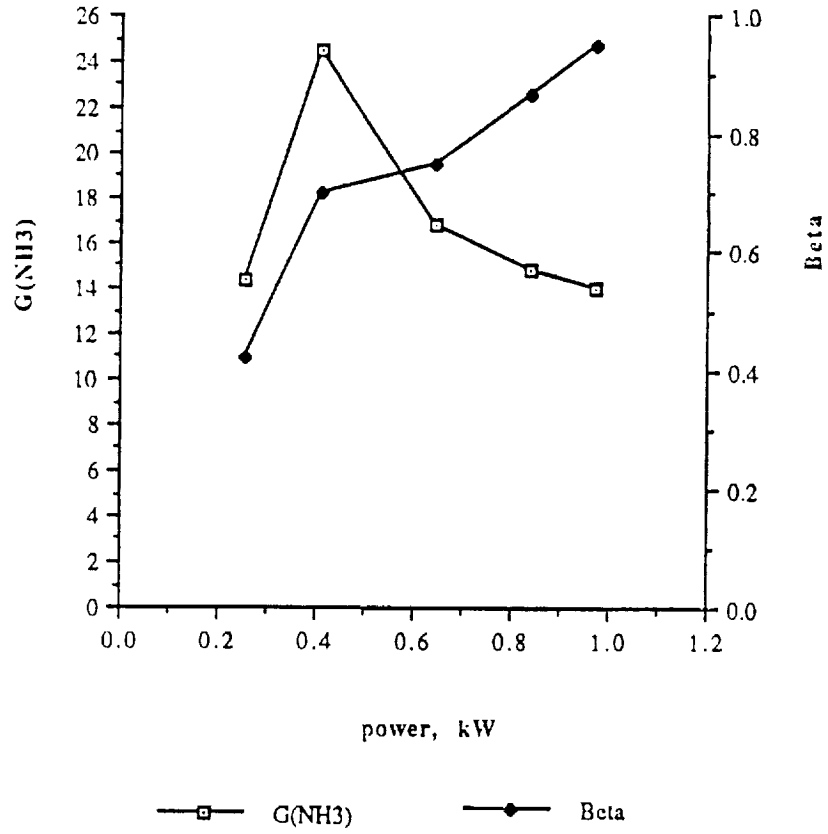


Figure 12: Ammonia, Flowrate 2 l/min, Pressure 7.5 Torr.

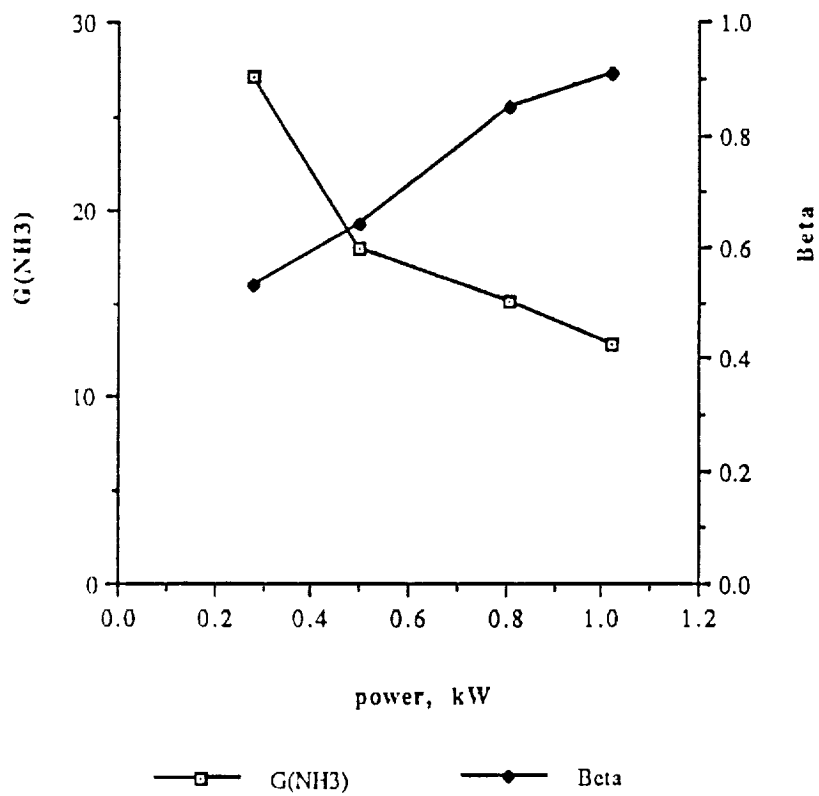


Figure 13: Ammonia, Flowrate 2 l/min, Pressure 10 Torr.

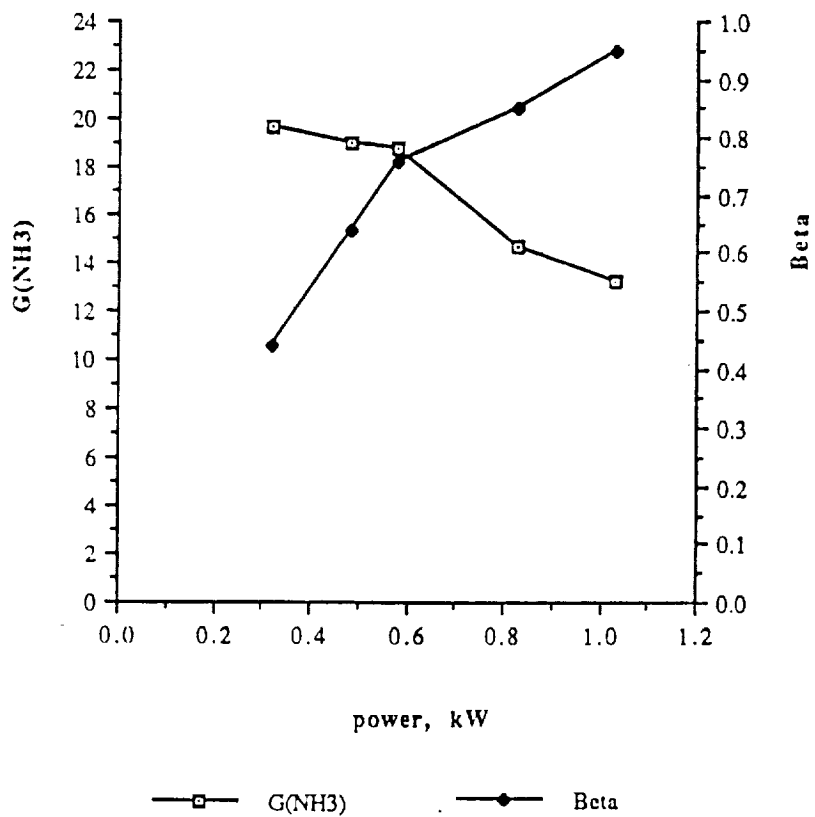


Figure 14: Ammonia, Flowrate 2 l/min, Pressure 15 Torr.

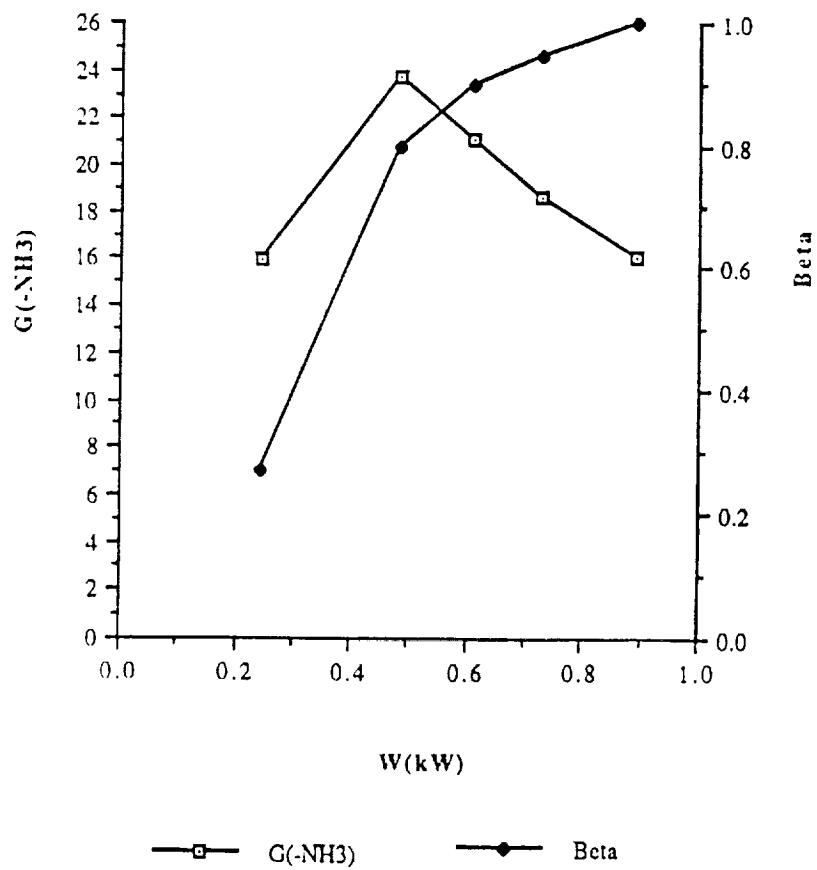


Figure 15: Ammonia, Flowrate 2 L/min, Pressure 20 Torr.

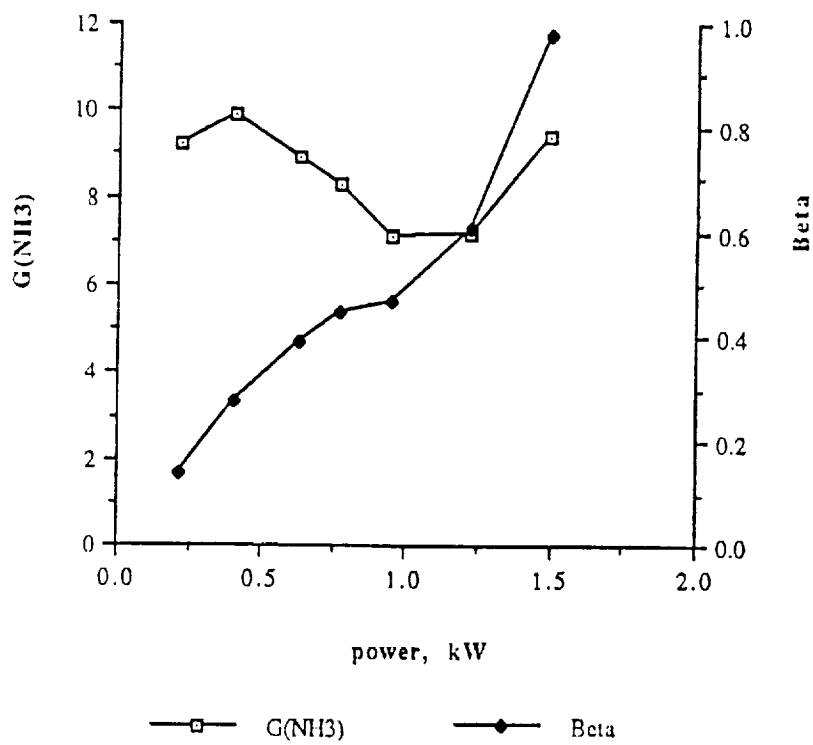


Figure 16: Ammonia, Flowrate 2 l/min, Pressure 25 Torr.

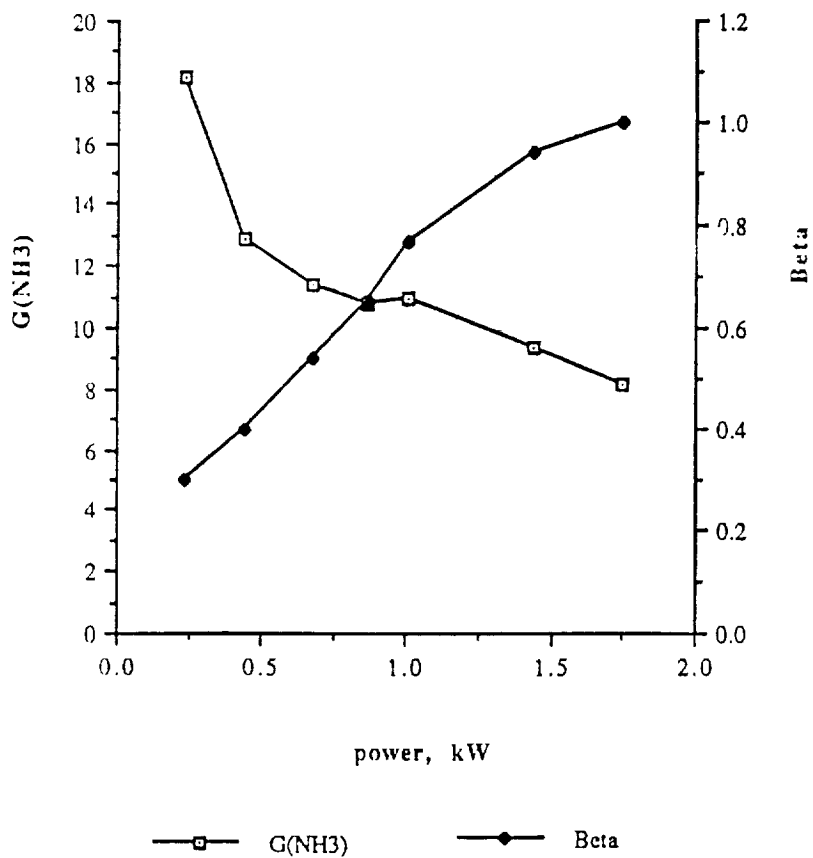


Figure 17: Ammonia, Flowrate 2 l/min, Pressure 30 Torr.

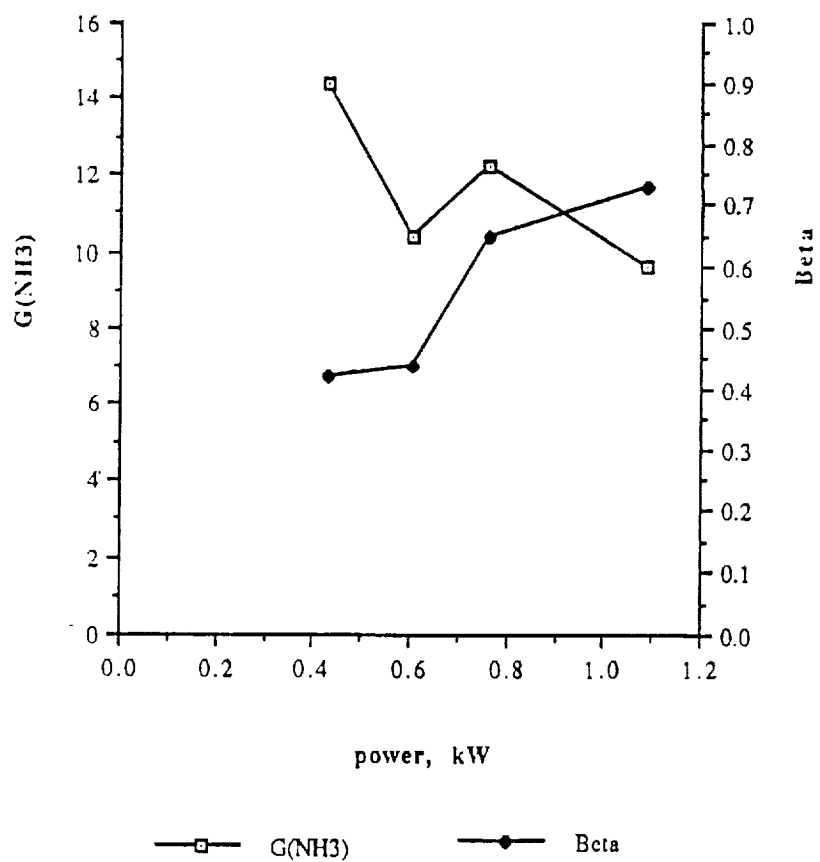


Figure 18: Ammonia, Flowrate 2 l/min, Pressure 40 Torr.

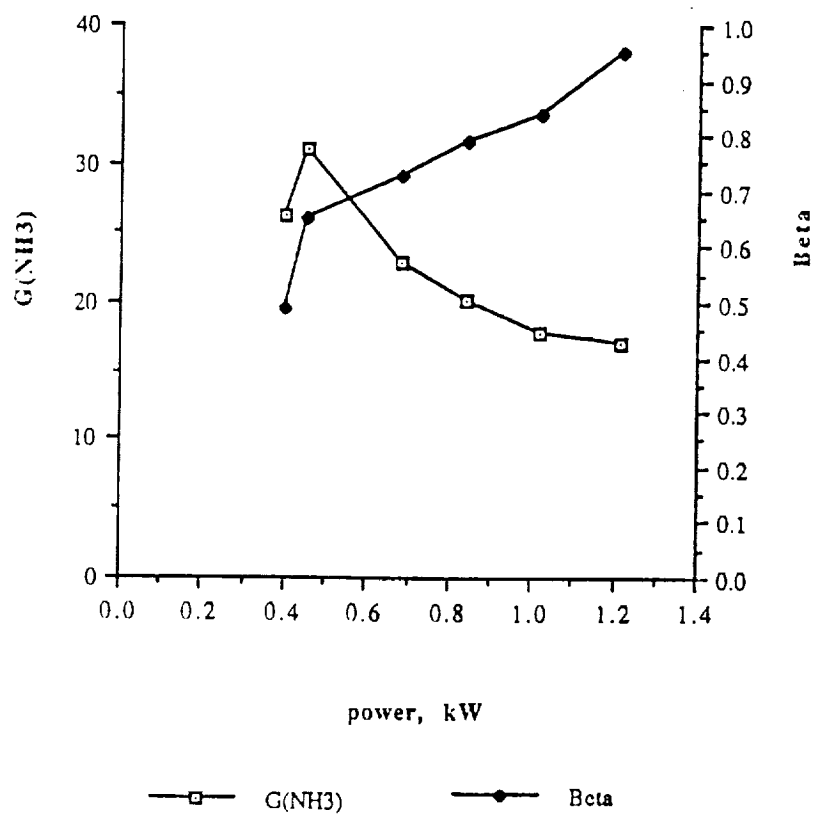


Figure 19: Ammonia, Flow-rate 3 l/min, Pressure 10 Torr.

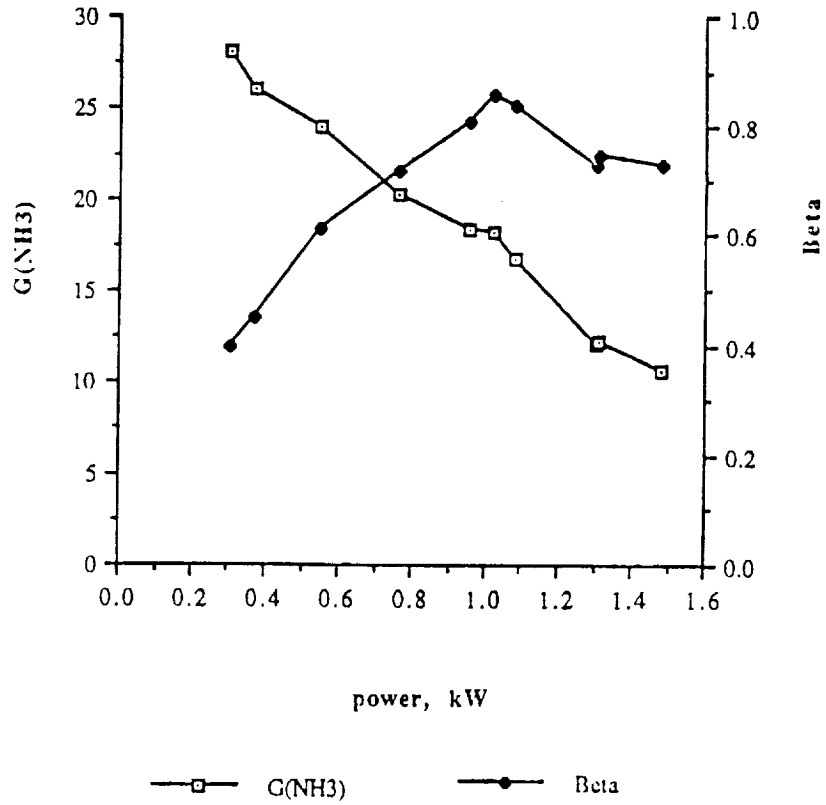


Figure 20: Ammonia, Flowrate 3 L/min, Pressure 15 Torr.

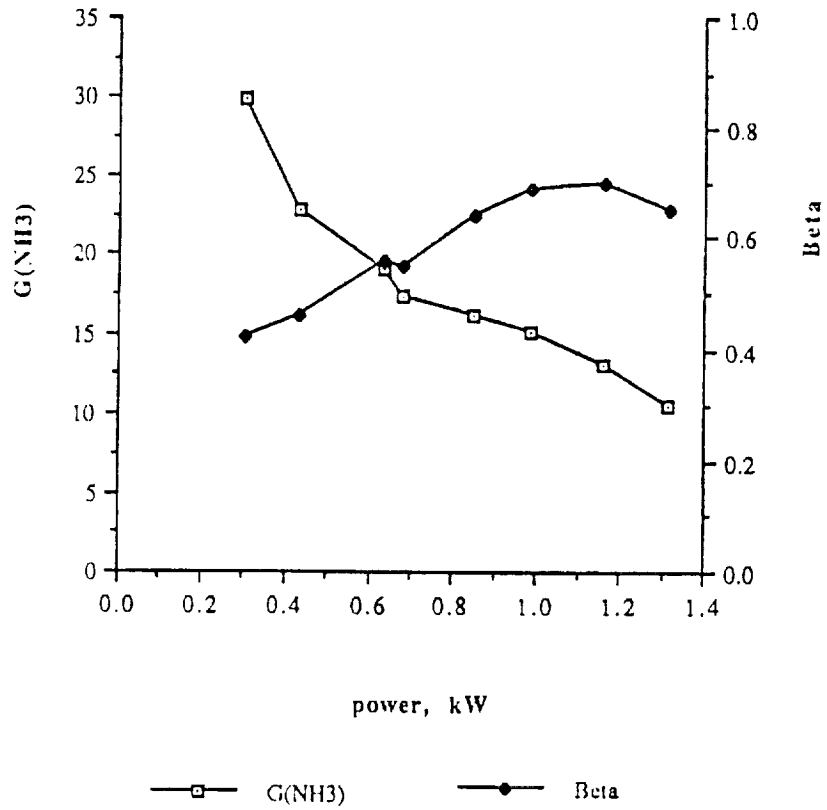


Figure 21: Ammonia, Flowrate 3 L/min, Pressure 20 Torr.

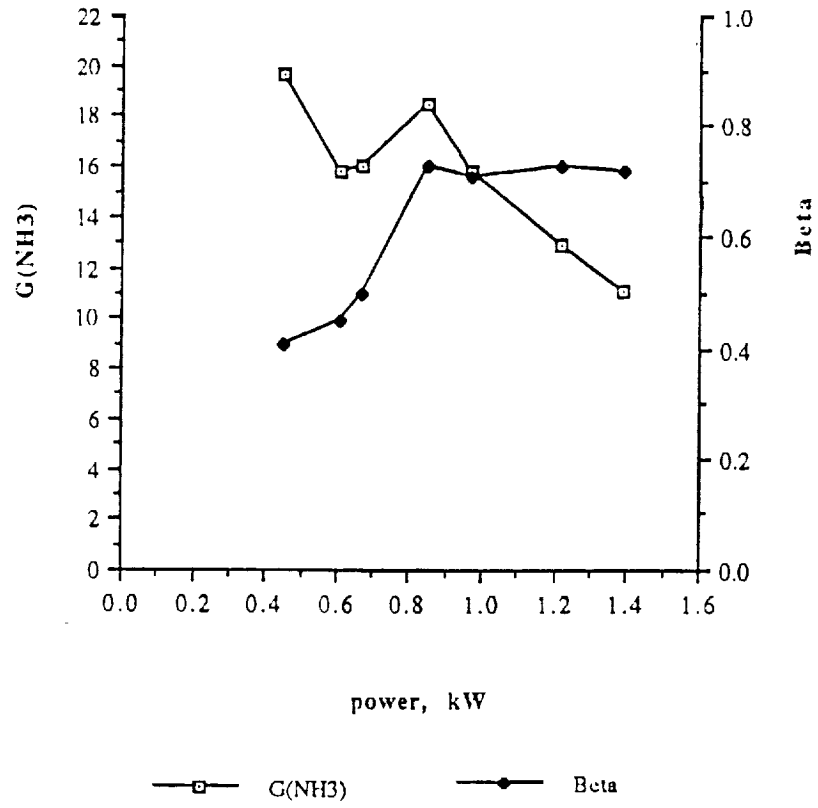


Figure 22: Ammonia, Flowrate 3 L/min, Pressure 25 Torr.

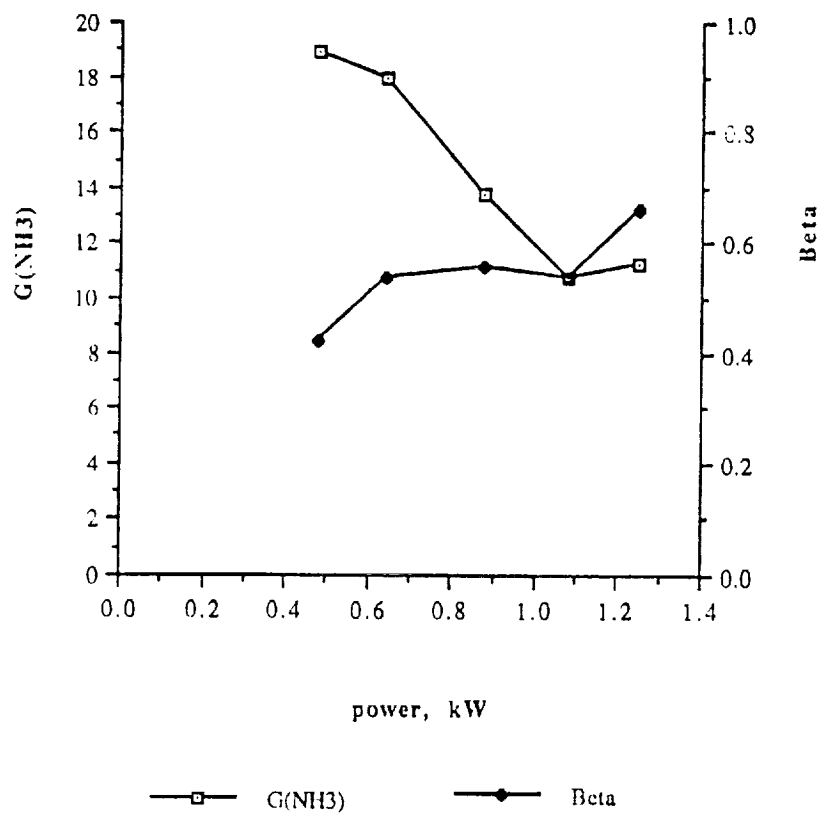


Figure 23: Ammonia, Flowrate 3 L/min, Pressure 30 Torr.

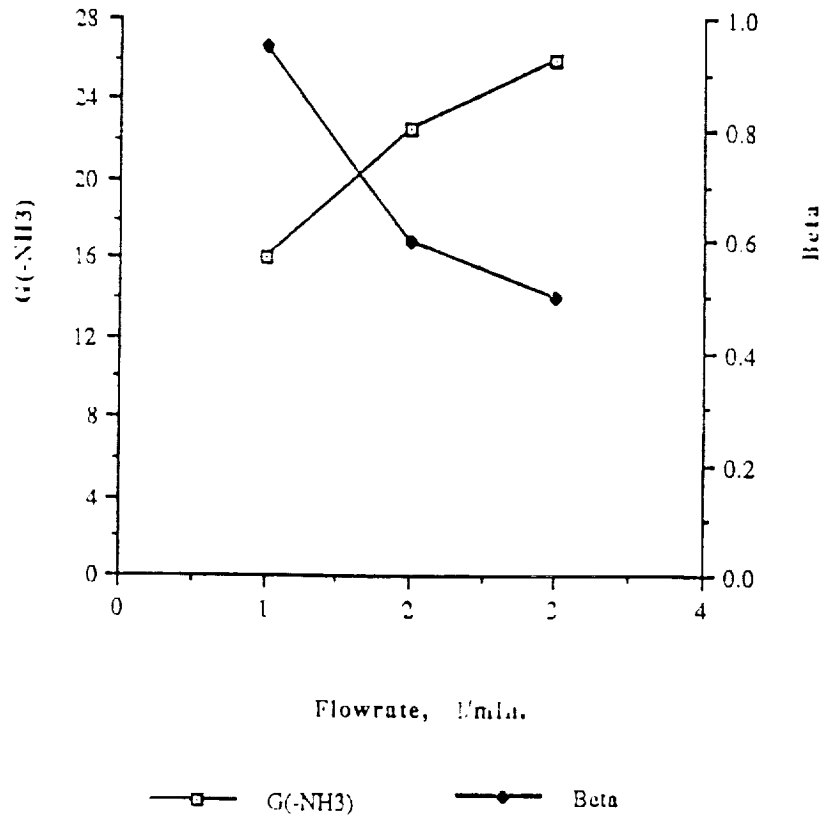


Figure 24: The Dependence of G-value and Beta for Ammonia on Flowrate. Pressure 10 Torr, Power 400 W.

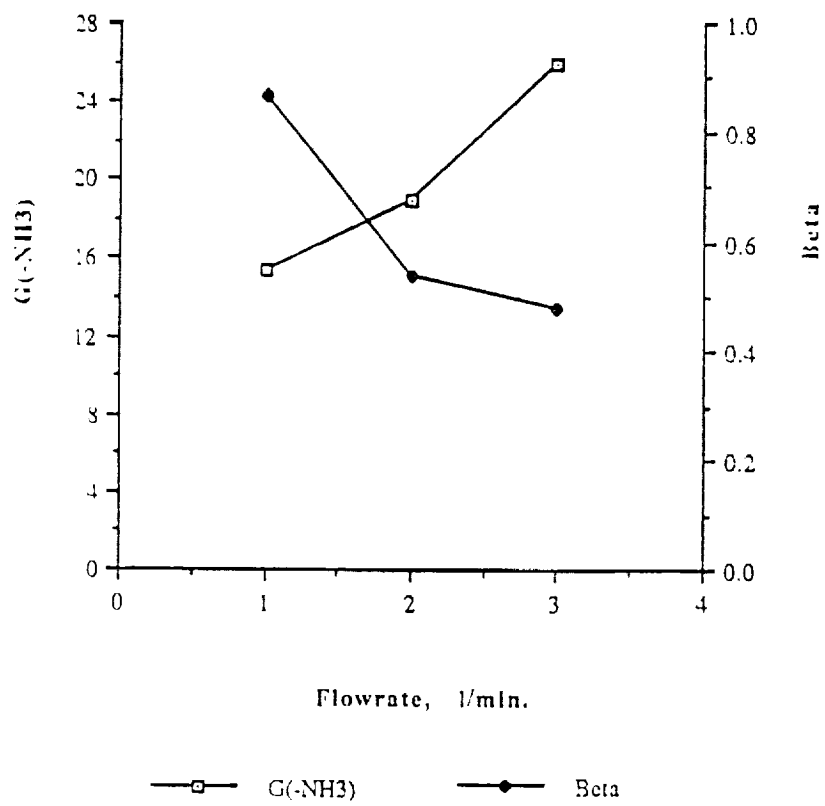


Figure 25: Ammonia, Pressure 15 Torr, Power 400 W.

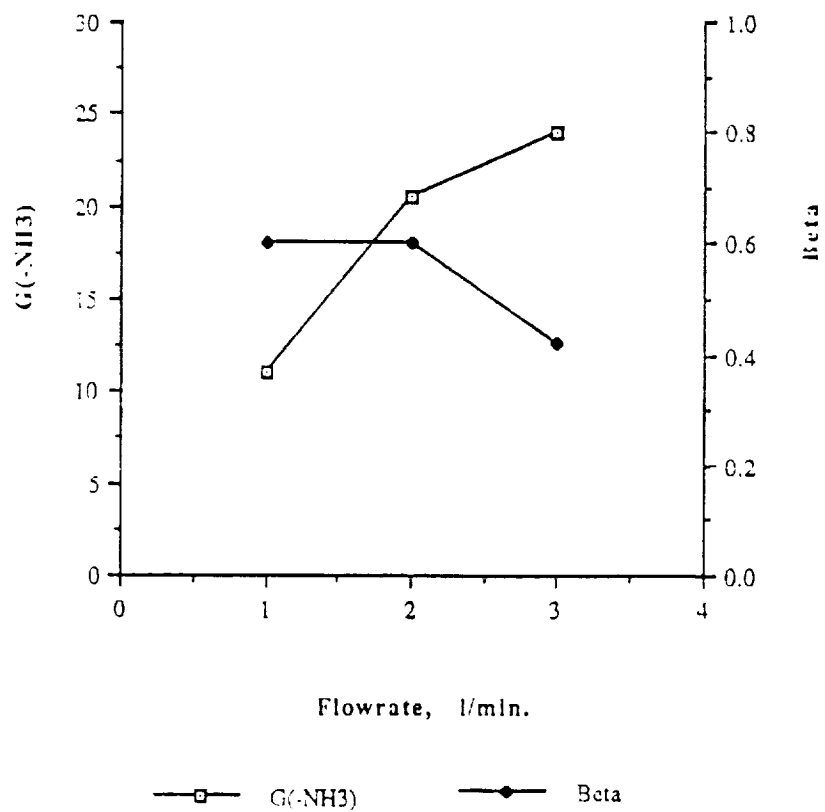


Figure 26: Ammonia, Pressure 20 Torr, Power 400 W.

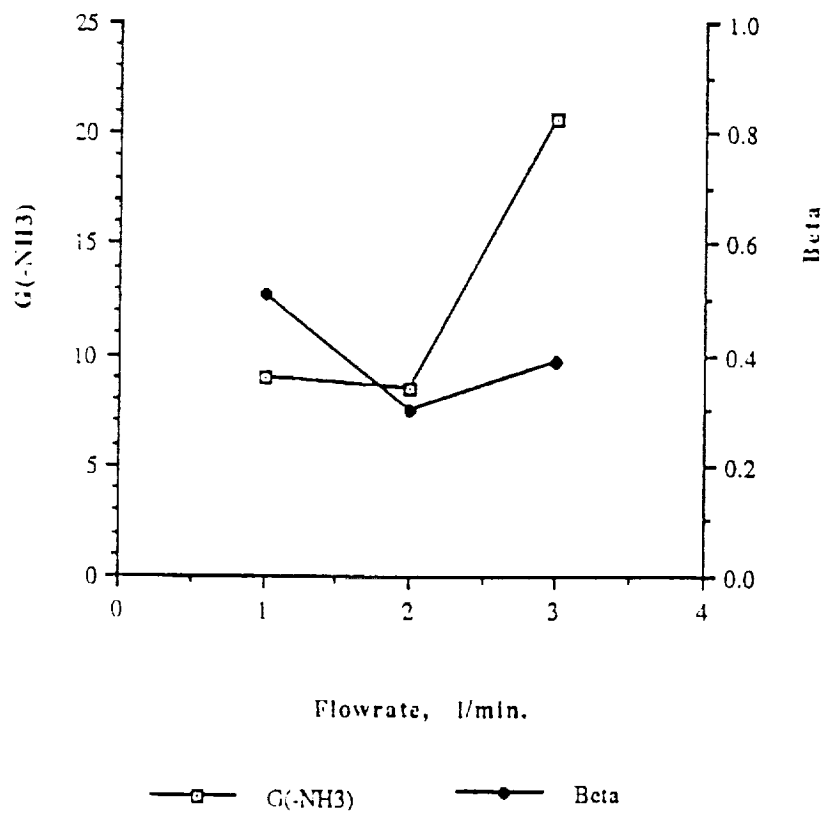


Figure 27: Ammonia, Pressure 25 Torr, Power 400 W.

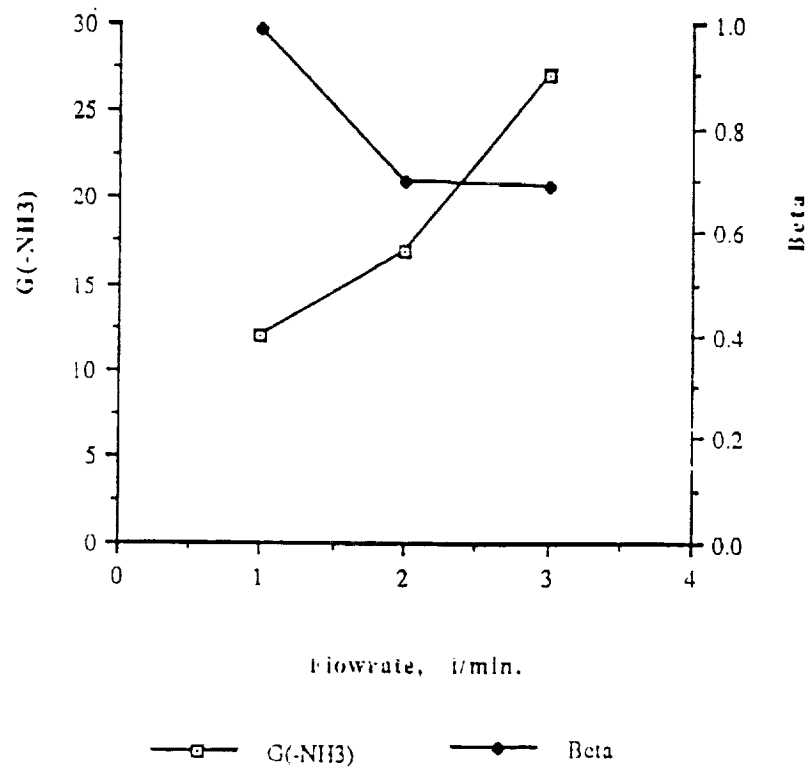


Figure 28: Ammonia, Pressure 10 Torr, Power 600 W.

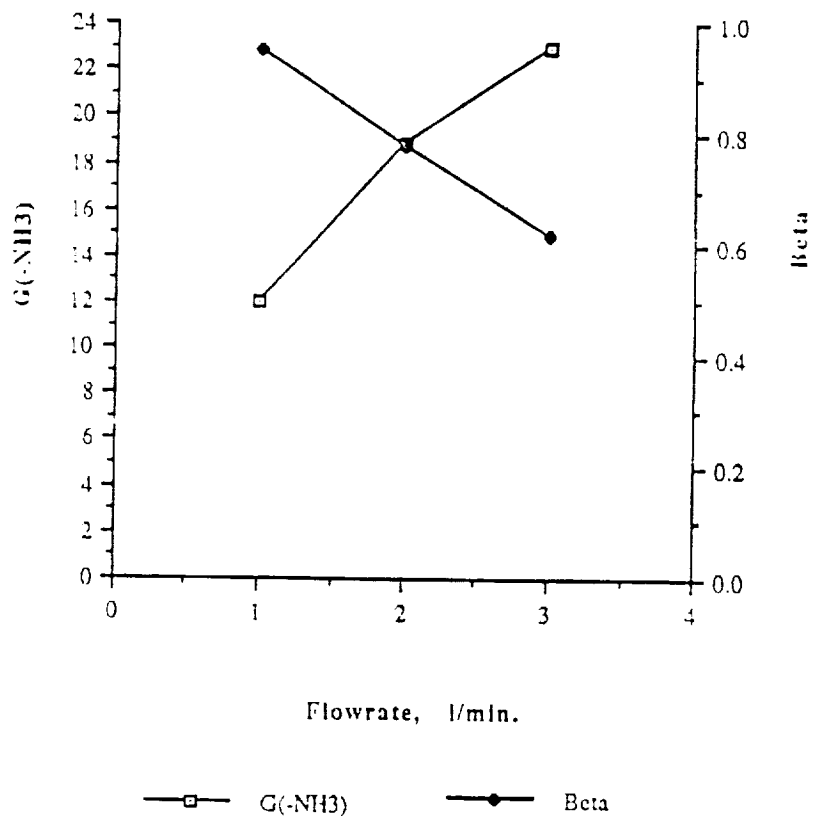


Figure 29: Ammonia, Pressure 15 Torr, Power 600 W.

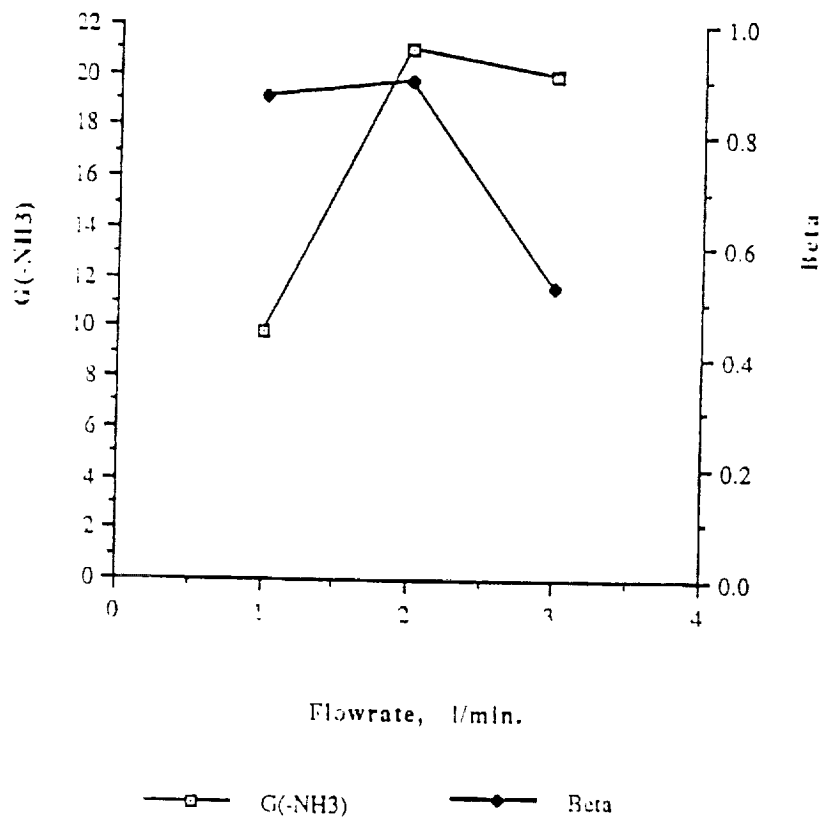


Figure 30: Ammonia, Pressure 20 Torr, Power 600 W.

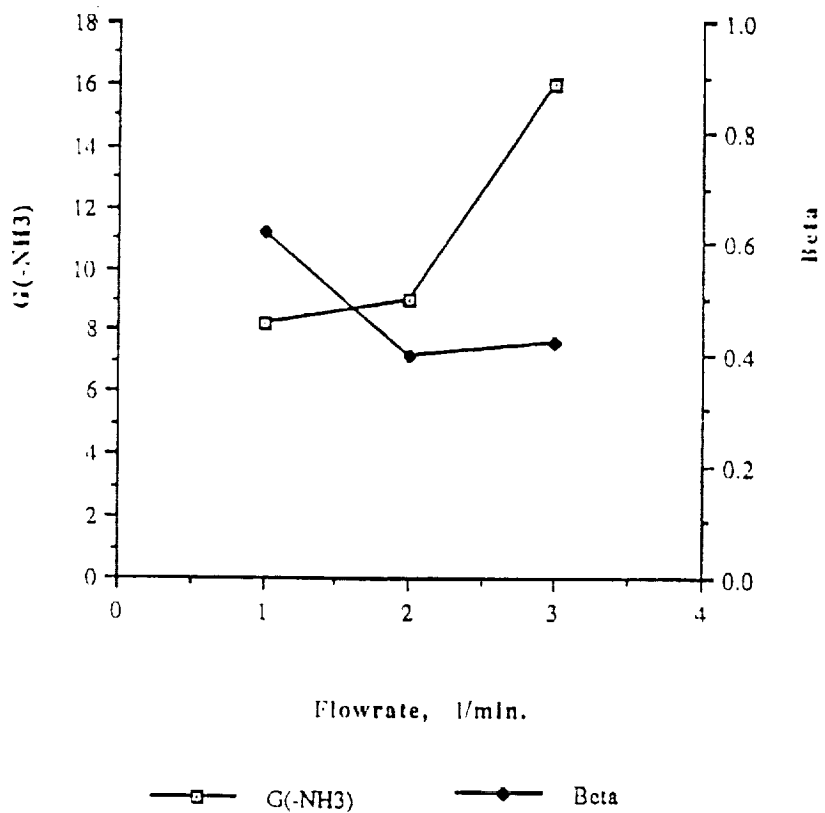


Figure 31: Ammonia, Pressure 25 Torr, Power 600.

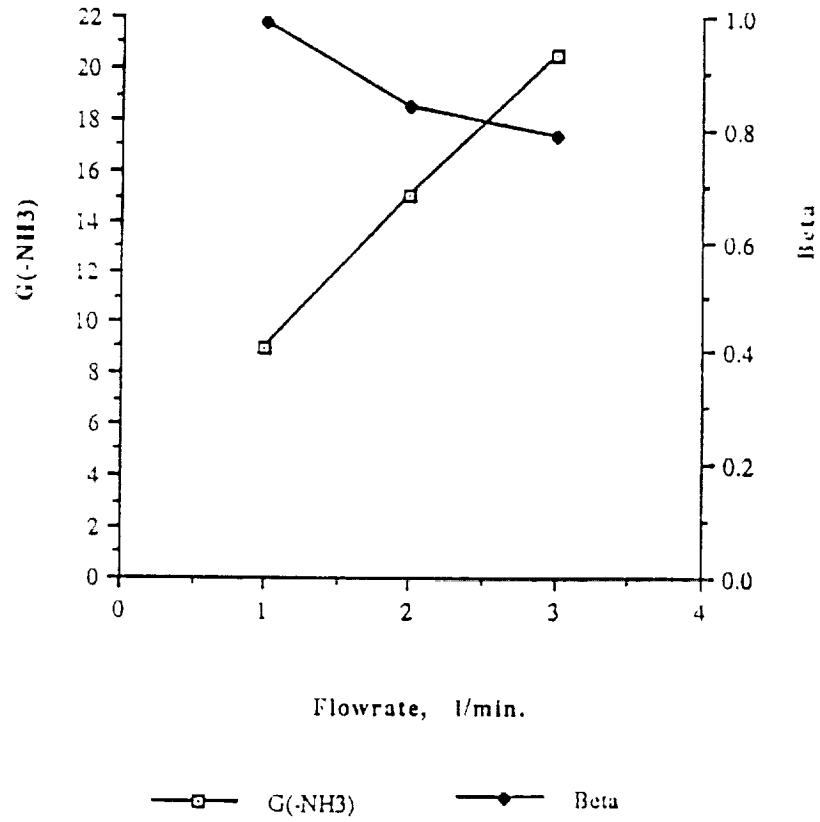


Figure 32: Ammonia, Pressure 10 Torr, Power 800 W.

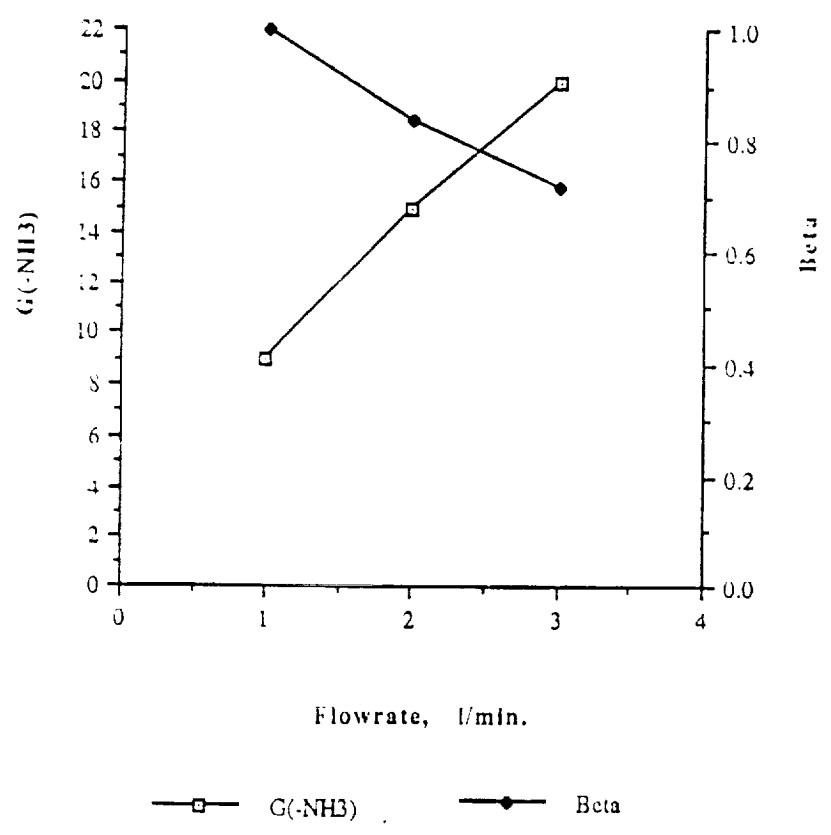


Figure 33: Ammonia, Pressure 15 Torr, Power 800 W.

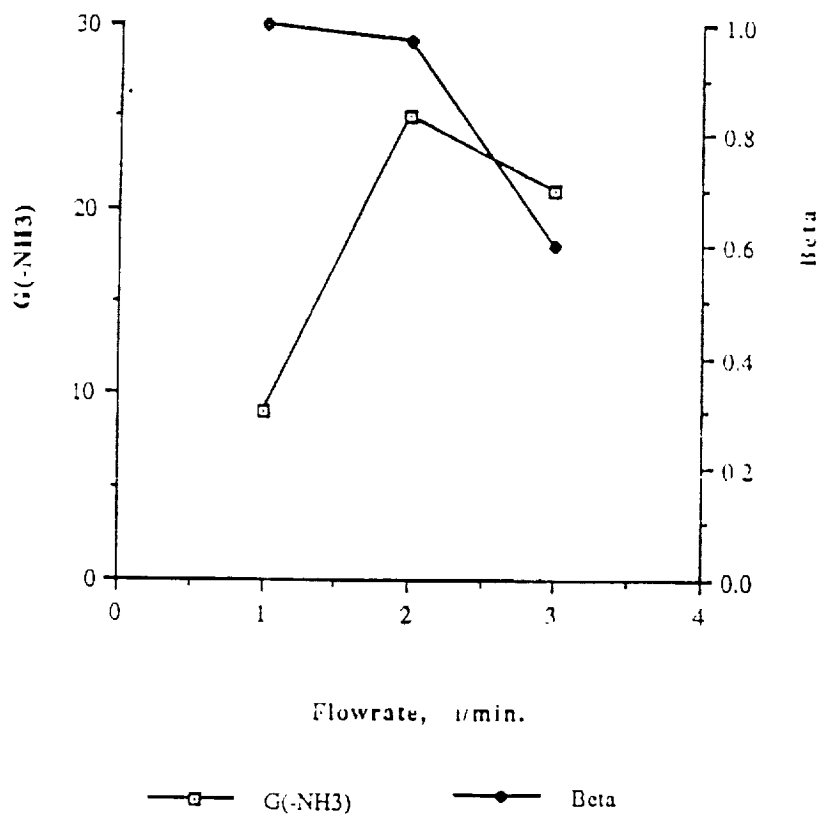


Figure 34: Ammonia, Pressure 20 Torr, Power 800 W

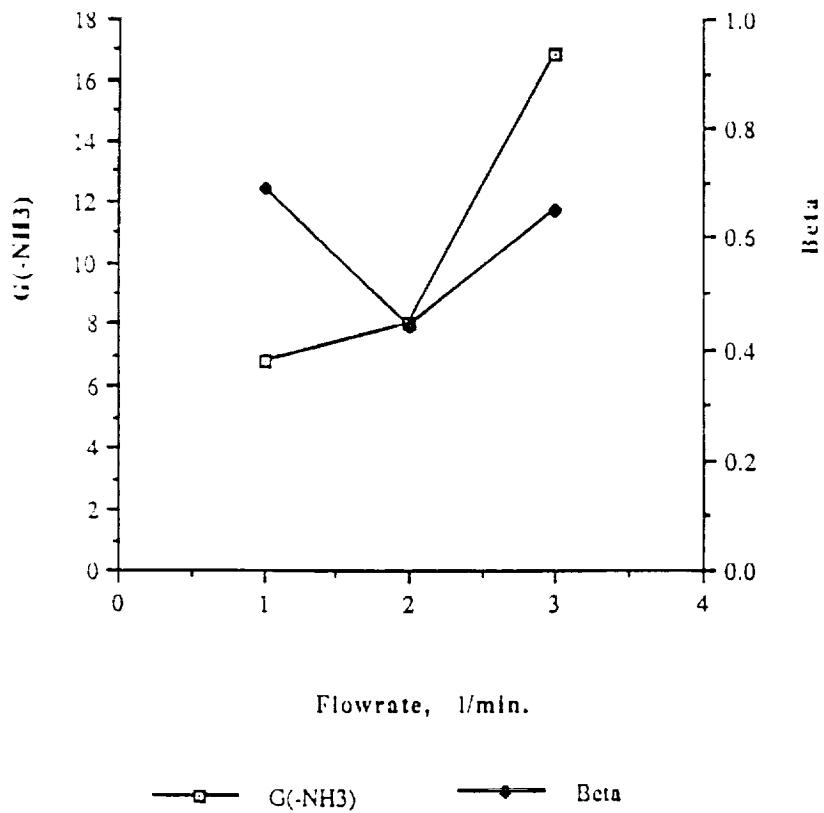


Figure 35: Ammonia, Pressure 25 Torr, Power 800 W.

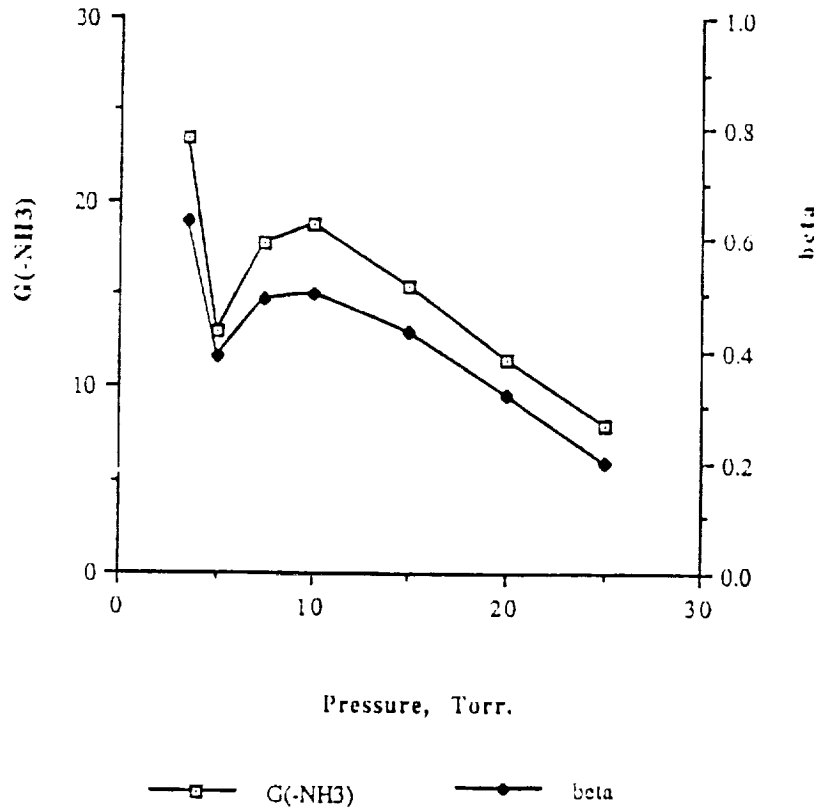


Figure 36: The Dependence of the G-value and Beta on Pressure. Ammonia, Flowrate 1 l/min, Power 200 W.

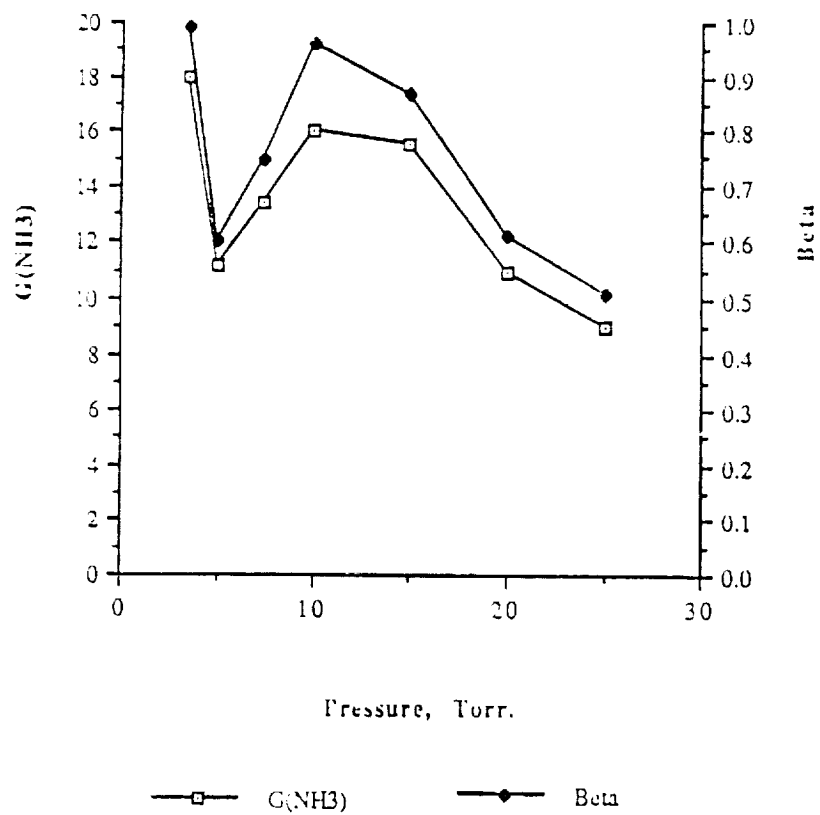


Figure 37: Ammonia, Flowrate 1 l/min, Power 400W.

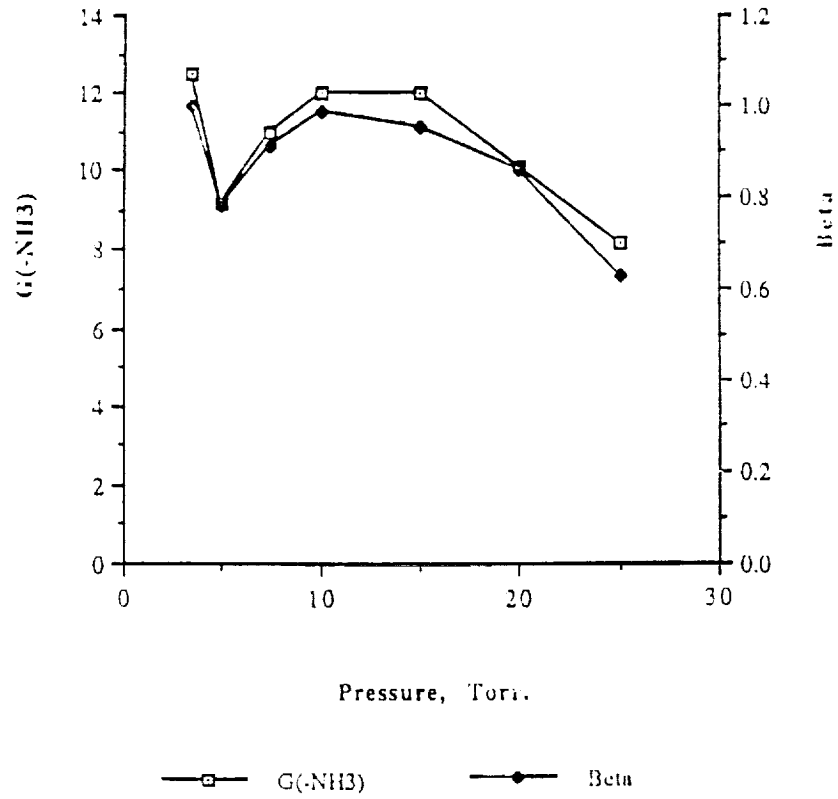


Figure 38: Ammonia, Flowrate 1 l/min, Power 600 W.

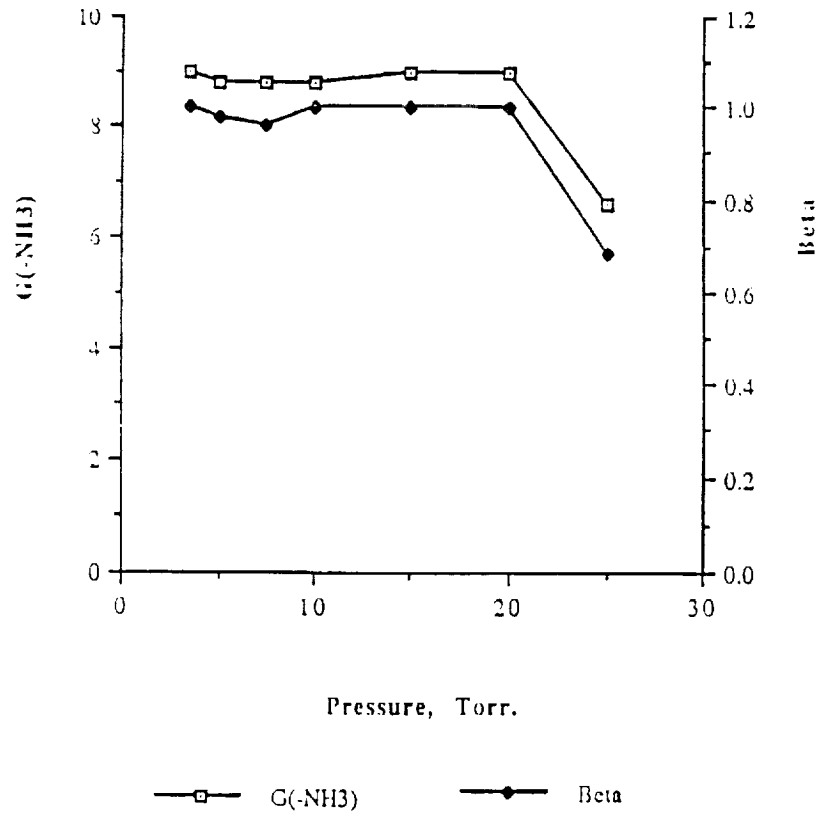


Figure 39: Ammonia, Flowrate 1 l/min, Power 800 W.

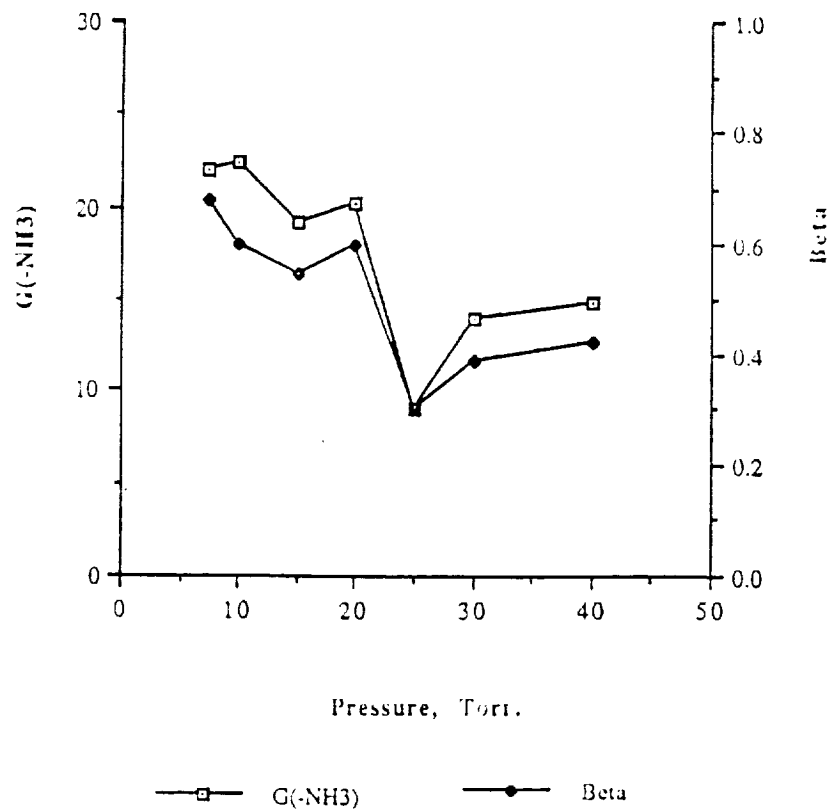


Figure 40: Ammonia, Flowrate 2 l/min, Power 400 W.

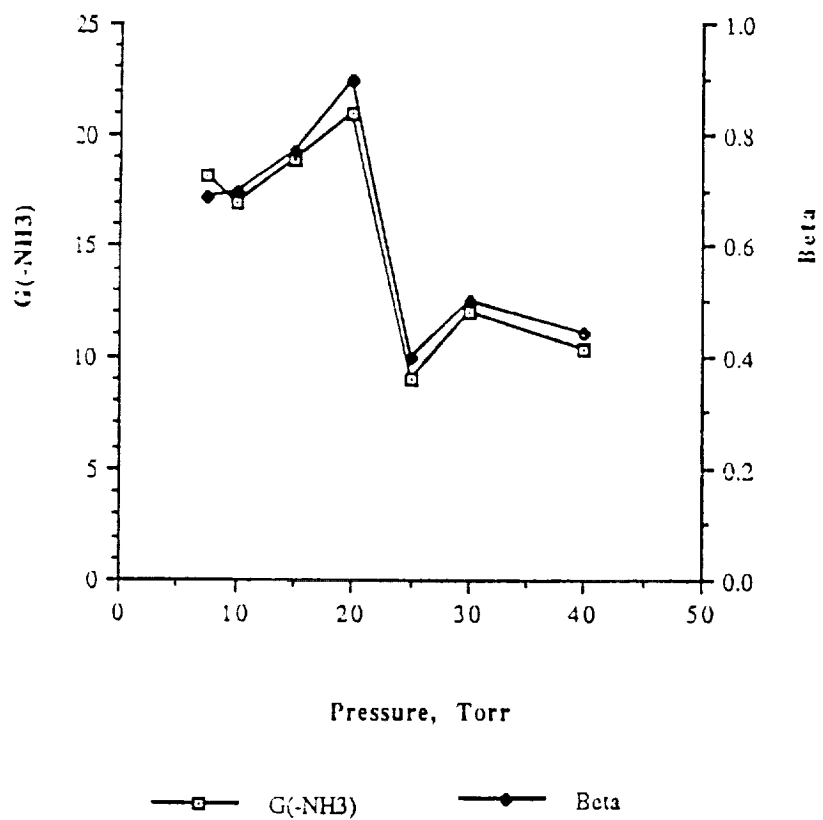


Figure 41: Ammonia, Flowrate 2 l/min, Power 600 W.

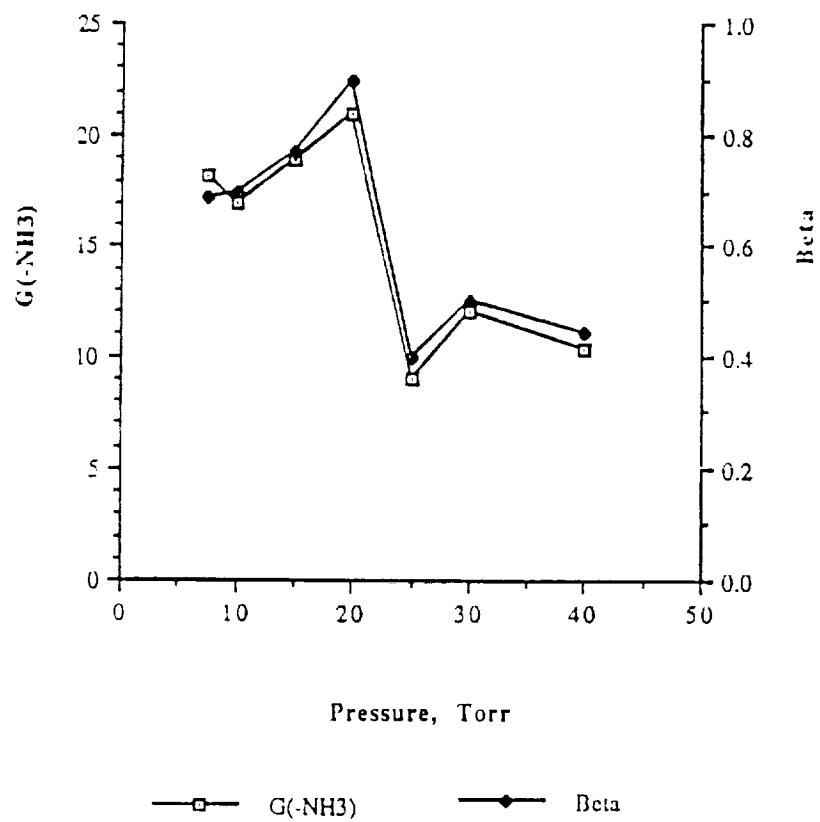


Figure 41: Ammonia, Flowrate 2 l/min, Power 600 W.

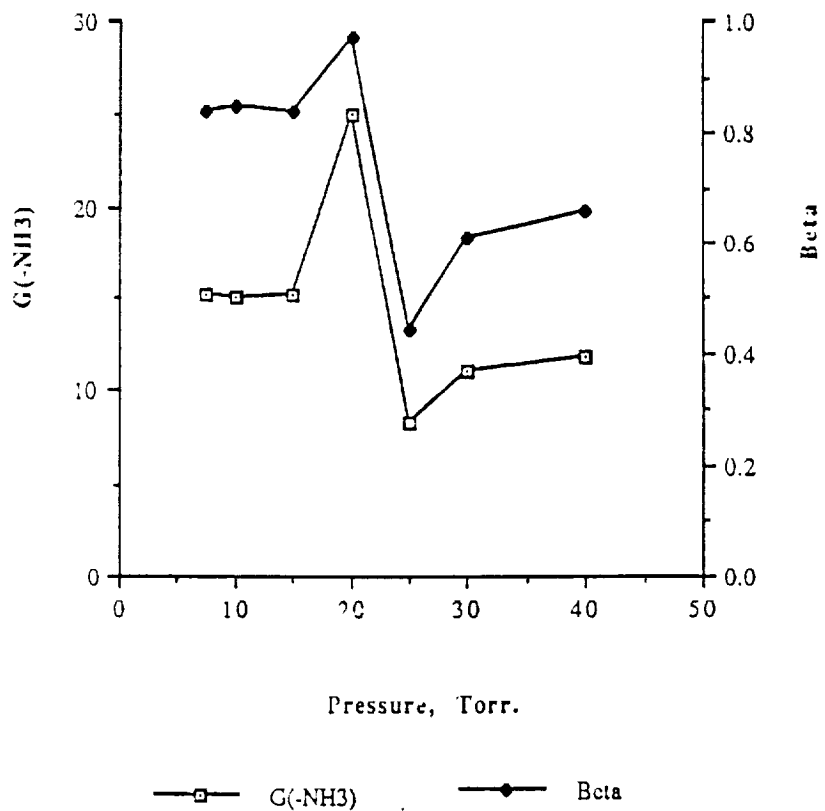


Figure 42: Ammonia, Flowrate 2 l/min, Power 800 W.

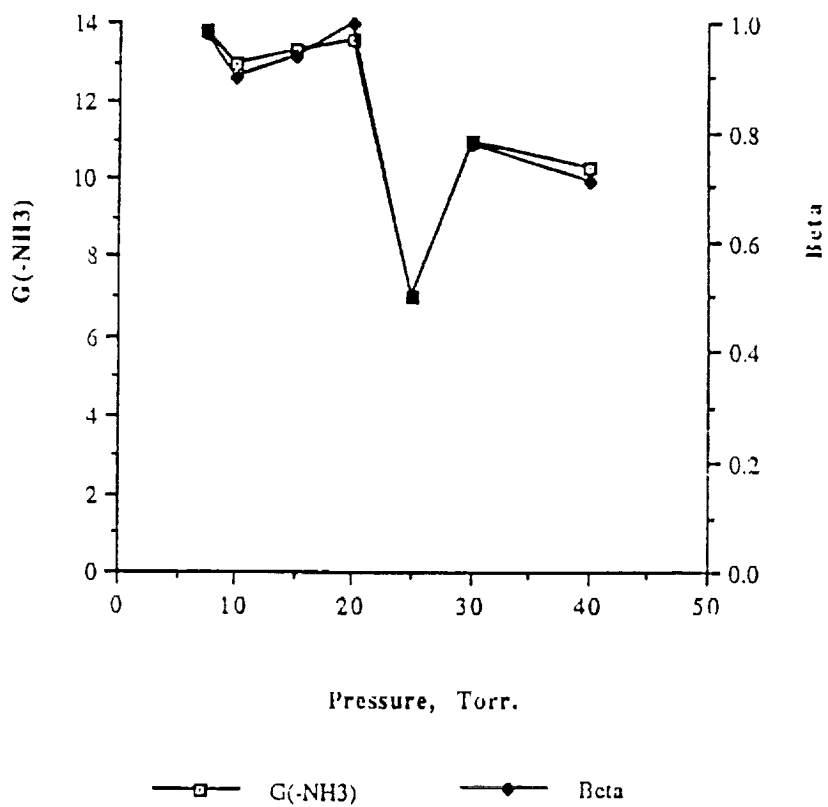


Figure 43: Ammonia, Flowrate 2 l/min, Power 1000 W.

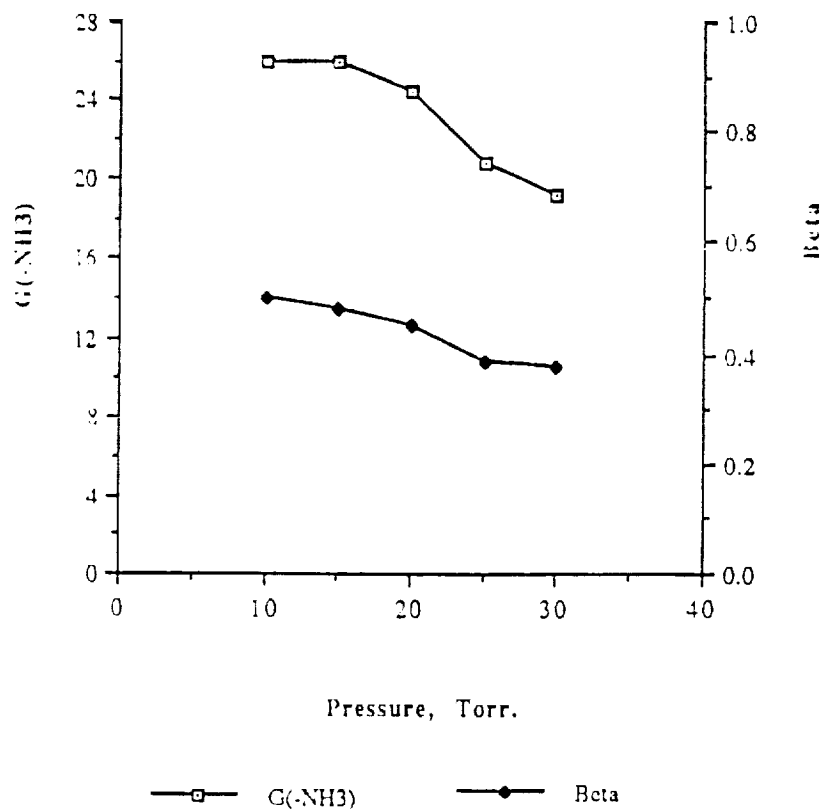


Figure 44: Ammonia, Flowrate 3 l/min, Power 400 W.

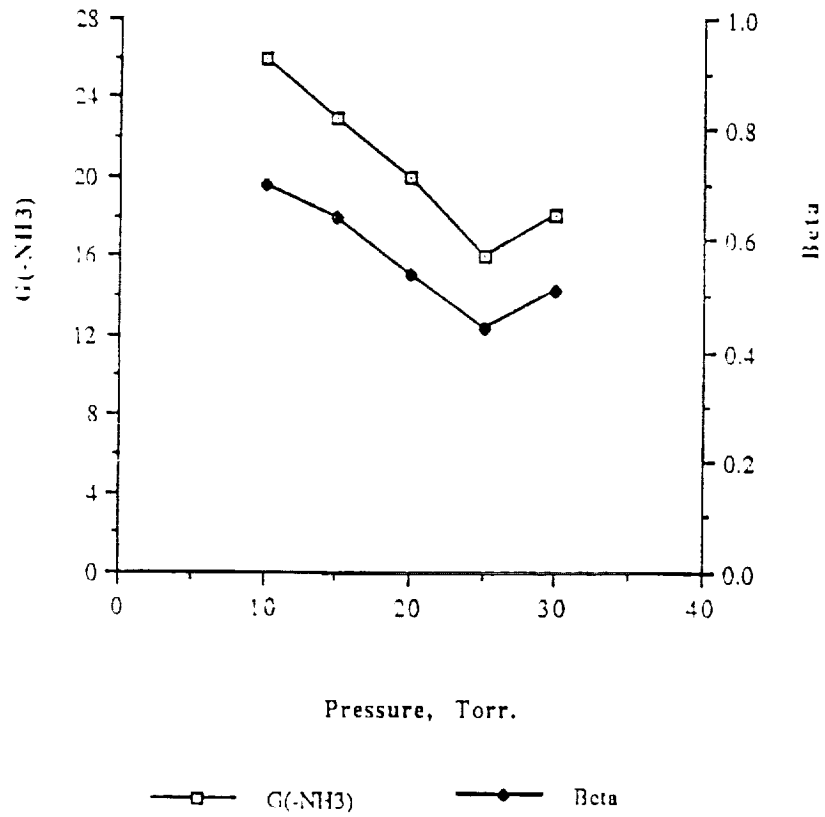


Figure 45: Ammonia, Flowrate 3 l/min, Power 600 W.

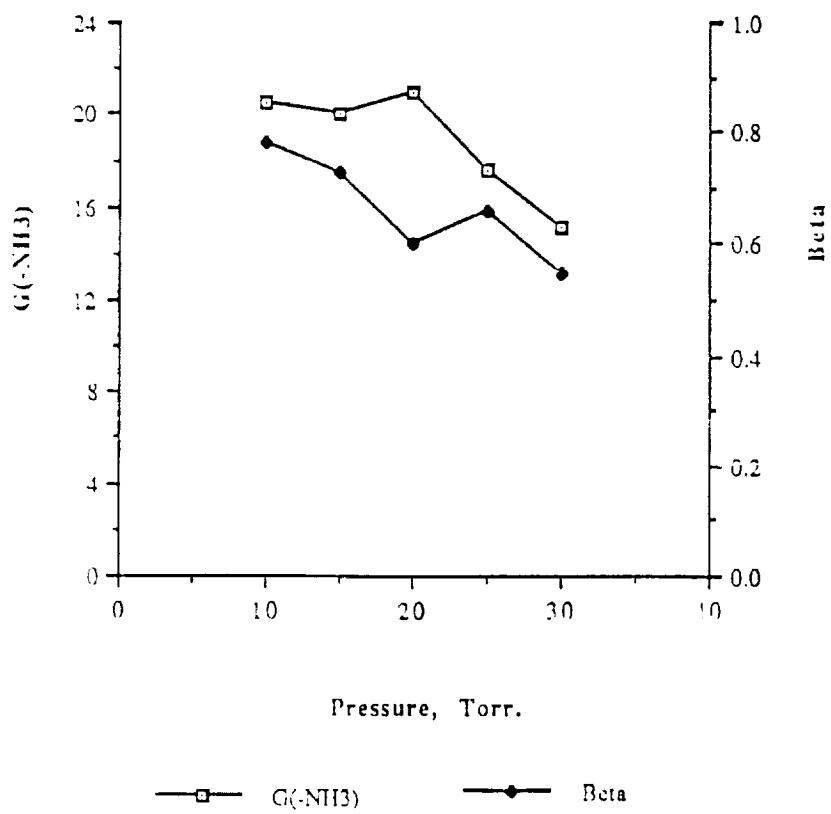


Figure 46: Ammonia, Flowrate 3 l/min, Power 800 W.

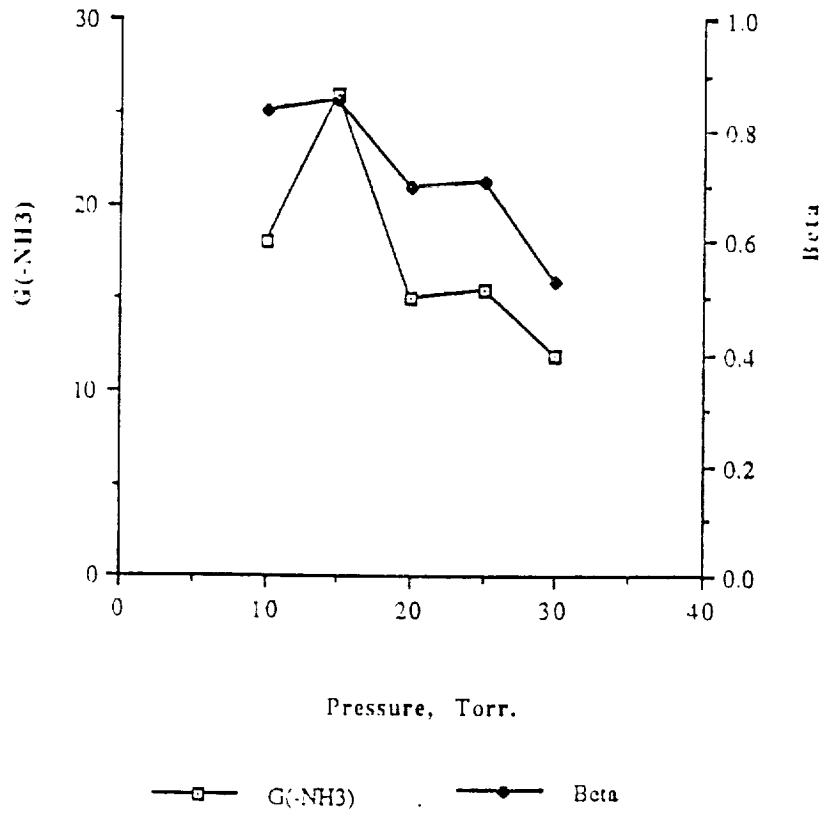


Figure 47: Ammonia, Flowrate 3 l/min, Power 1000 W.

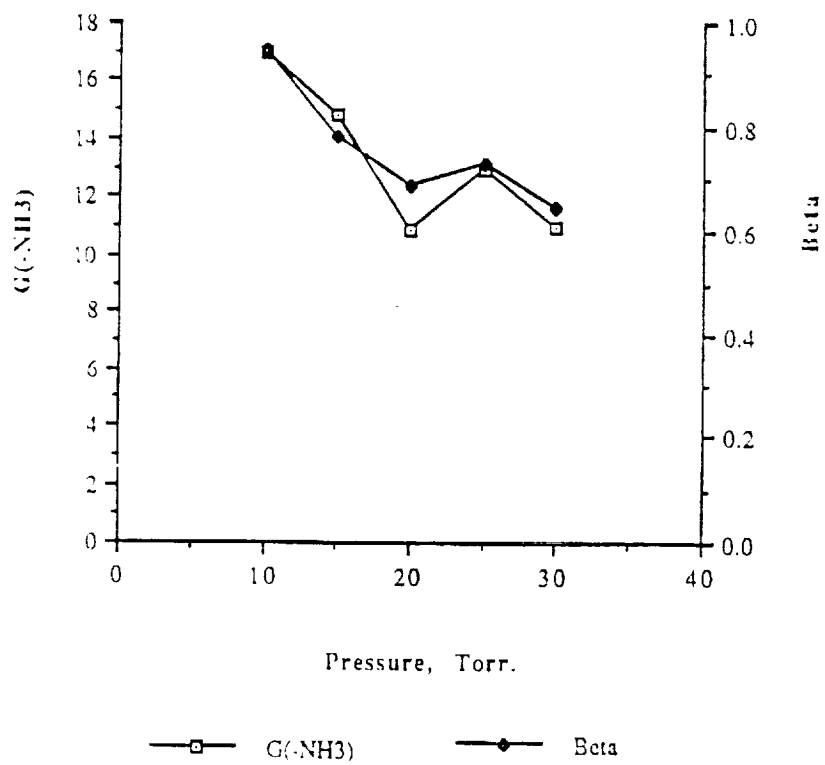


Figure 48: Ammonia, Flowrate 3 l/min, Power 1200 W.

### Nitrous Oxide.

An on-going study of the plasma decomposition of  $N_2O$  is proceeding. This investigation has been somewhat more difficult than that for ammonia due in the first instance to the difficulty of maintaining a steady-state plasma. The stable plasma formation appears to be highly dependent on both flowrate and input power, with the plasma abruptly moving from the steady-state to a pulsing mode. This may arise from the low power levels available and the fact that  $N_2O$  is a well known scavenger of electrons. Secondly, the by-products are much more complicated, with the condensible products now include at least  $NO$ ,  $NO_2$  as well as the remaining  $N_2O$  and the non-condensable  $N_2$  and  $O_2$ .

As they are warmed, the products condensed by the  $LN_2$  traps go from a dark green solid to a blue liquid to first a clear gas and then, as the temperature rises, a brown gas. An interesting observation is that upon re-cooling back down to  $LN_2$  temperature the gas condenses back to a blue, not green, solid. This result suggests the presence of radicals in the original sample that react as the trap warms up to room temperature. It is hoped to undertake a spectroscopic study to investigate the underlying processes.

At the flowrates and power levels covered (0.5-0.75 l/min, 650-1000 W) we have found the G-value of  $N_2O$  to lie in the range of 3-6 molecules/100 eV. This result is in reasonable agreement with the radiation G-values of 3.0-8.8 molecules/100 eV. Further work at higher flowrates and input power is necessary to complete this study.

### Methane.

A brief study of the decomposition of methane was also undertaken. Preliminary studies indicated a very complex problem with the production of numerous by-products.

Upon the introduction of methane, the matching unit had to be slightly re-tuned to achieve optimum coupling of power into the plasma. With the formation of the methane discharge the plasma is a very luminous bluish purple. The methane plasma rapidly forms a thin yellowish-brown polymer on the inside of the plasma tube, the production rate of

which appeared to be highly dependent on the operating conditions. Initial experiments to identify this product indicated a highly cross-linked polymer.

The products condensed in the LN<sub>2</sub> traps were found to include ethane, butane, propane, acetylene, benzene, 2-methyl propane. Additional nonvolatile higher order hydrocarbons were found clinging to the trap following the warm-up to room temperature.

### **Conclusions.**

Ammonia, nitrous oxide, and methane all may be easily decomposed in an inductively coupled plasma operating at 13.56 MHz and at power levels up to 2.5 kW.

In the case of ammonia, which we studied most extensively,  $G(-\text{NH}_3)$  varied from 6.0 to 32.0 molecules/100 eV, depending upon conditions. In terms of specific energy efficiency, which is the reciprocal of  $G(-\text{NH}_3)$  and which is best expressed in engineering units, this corresponds to a range of 0.45 to 0.084 kWhr/mole. This energy requirement would seem to be well within the capabilities of power supplies designed for use in space.

Inductively coupled plasmas are more effective than capacitatively plasmas or ionizing radiation in destroying ammonia. The G-value for ammonia destruction in a capacitatively coupled discharge depends upon conditions but lies in the range of 6 - 20 molecules/100 eV. Radiation chemistry values for  $G(-\text{NH}_3)$  lie in the range of 2.7 - 10 molecules/100 eV and are independent of whether the incident radiation is alpha, beta, or gamma. Although lower, the radiation G-values can serve as a conservative estimator of the plasma G-values.

Nitrous oxide was decomposed our plasma with a  $G(-\text{N}_2\text{O})$  ranging between 3.0 and 8.8 molecules/100 eV. Hence, N<sub>2</sub>O is less easily destroyed than NH<sub>3</sub>.

We have also showed [30] (See Appendix for a reprint) that the G-value for an arbitrary reaction can be calculated theoretically from a knowledge of the electron velocity distribution, the various electron-molecule scattering cross sections, and the rate constants

for secondary reactions. This result is fundamental, since it permits both plasma chemistry and radiation chemistry to be put on a common theoretical foundation.

### References.

- 1) C. H. Chang and E. Pfender, *Plasma Chem. Plasma Process.* **10**, 473 (1990).
- 2) C. H. Chang and E. Pfender, *Plasma Chem. Plasma Process.* **10**, 493 (1990).
- 3) J. Mostaghimi, P. Proulx and M. I. Boulos, *J. Num. Heat Transfer.* **8**, 187 (1985).
- 4) J. Mostaghimi, P. Proulx and M. I. Boulos, *Plasma Chem. Plasma Process.* **4**, 199 (1985).
- 5) T. Harada, T. Yoshida, T. Koseki and K. Akashi, *J. Jpn. Inst. Met.* **45**, 1138 (1981).
- 6) G. Y. Zhao, Y. Wang and C. W. Zhu, *Acta Mech. Sin.* **4**, 124 (1988).
- 7) G. Y. Zhao and C. W. Zhu, *IEEE Trans. Plasma Sci.* **PS-14**, 531 (1986).
- 8) G. Y. Zhao, J. Mostaghimi and M. I. Boulos, *Plasma Chem. Plasma Process.* **10**, 133 (1990).
- 9) G. Y. Zhao, J. Mostaghimi and M. I. Boulos, *Plasma Chem. Plasma Process.* **10**, 151 (1990).
- 10) J. Mostaghimi and M. Boulos, *Plasm. Chem. Plasm. Proc.* **9**, 25 (1989).
- 11) M. Boulos and R. M. Barnes, Inductively Coupled Plasma Spectroscopy, Part 2. P. W. J. M. Boumans, Editor. Wiley, New York (1987). C9 pp289-352.
- 12) P. Yank, R. M. Barnes, J. Mostaghimi and M. I. Boulos, *Spectrochim. Acta* **44B**, 657 (1984).
- 13) S. L. Girshick and W. Yu, *Plasm. Chem. Plasm. Proc.* **10**, 515 (1990).
- 14) G. A. Luk'yanov, V.V. Nazarov and V.V. Sakhin, *Sov. Phys.-Tech. Phys.* **23**, 744 (1978).
- 15) H. D. Steffens and K. H. Busse, *Proc of ISPC-7.* **1**, 710 (1985).
- 16) G. Frind, C. P. Goody and L. E. Prescott, *Proc of ISPC-6.* **1**, 120 (1983)
- 17) Y. Arata, A. Kobayashi and Y. Habara, *Jpn. J. Appl. Phys.* **1**, 1697 (1986).
- 18) R. Hidaka, T. Ooki, K. Takeda, K. Konda, H. Kanda, K. Chino, Y. Matsuda, K. Muraoka and M. Akazaki, *Jpn. J. Appl. Phys.* **26**, L1724 (1987).
- 19) R. d'Agostino, F. Cramarossa, S. De Benedictis and G. Ferraro, *Plasm. Chem. Plasm. Proc.* **1**, 19 (1981).
- 20) R. Platzman, *Radiation Res.* **17**, 419 (1962).

- 21) For example, J. D. Craggs and H. S. W. Massey, *The Collisions of Electrons with Molecules* in Handbuch der Physik, S. Flugge, Editor, Springer-Verlag, Berlin, 1959. 37-1, pp.167-187.
- 22) M. Burton and K. Funabashi, *Adv. Chem. Ser.* **80**, 140, (1964).
- 23) H. Wiener and M. Burton, *J. Am. Chem. Soc.* **75**, 5815 (1953).
- 24) A. J. Swallow, *Radiation Chemistry of Organic Compounds*, Pergamon Press, Oxford, 1960. p.56.
- 25) A. Kupperman and M. Burton, *Rad. Res.* **10**, 636 (1959).
- 26) R. E. Honig and C. W. Sheppard, *J. Phys. Chem.* **50**, 119 (1946).
- 27) P. Fauchais and J. Rakowitz, *J. de Physique, Colloque C7, supplement au No. 7 Tome 40*. Page 7, July 1979.
- 28) A. T. Bell, *Fundamentals of Plasma Chemistry*, Chap 1 in J. R. Hollahan and A. T. Bell, eds., Techniques and Applications of Plasma Chemistry, (John Wiley and Sons, New York, 1974).
- 29) A. M. Mearns and A. J. Morris, *CEP Symp. Ser.* **112**, 37 (1971).
- 30) J. K. Baird, G. P. Miller and N. Li, *J. Appl. Phys.* **68**, 3661 (1990).
- 31) G. P. Miller and J. K. Baird, unpublished.
- 32) D. B. Peterson, The Radiation Chemistry of Gaseous Ammonia. NSRDS-NBS **44**, (U.S. Department of Commerce, Washington, DC, 1974).
- 33) M. Kushner, private communication, 1989.
- 34) A. R. Anderson, Fundamental Processes in Radiation Chemistry, ed. P. Ausloos. Chap 5. (Interscience Publishers, John Wiley and Sons, New York, 1968).
- 35) K. Laidler, Chemical Kinetics, 3rd Edition, Harper and Row, New York, 1987.
- 36) J. E. Nicholas, A. I. Spiers and N. A. Martin, *Plasm. Chem. Plasm. Proc.* **6**, 39 (1986).
- 37) M. E. Fraser, D. A. Fee and R. S. Sheinson, *Plasm. Chem. Plasm. Proc.* **5**, 163 (1985).
- 38) M. Brossa and E. Pfender, *Plasm. Chem. Plasm. Proc.* **8**, 75 (1988).
- 39) R. N. Rudolph and J. H. Moore, *Plasm. Chem. Plasm. Proc.* **10**, 451 (1990).
- 40) H. Uyama and O. Matsumoto, *Plasm. Chem. Plasm. Proc.* **9**, 13 (1989).
- 41) H. Uyama and O. Matsumoto, *Plasm. Chem. Plasm. Proc.* **9**, 421 (1989).

- 42) N. Hershkowitz, M. H. Cho, C. H. Nam and T. Intrator, *Plasm. Chem. Plasm. Proc.* **8**, 35 (1988).
- 43) R. d'Agostino, F. Cramarossa, S. De Benedictis and F. Fracassi, L. Laska and K. Masek, *Plasm. Chem. Plasm. Proc.* **5**, 239 (1985).
- 44) A. Pastol and Y. Catherine, *J. Phys. D: Appl. Phys.* **23**, 799 (1990).
- 45) W. Andersen, B. Zwolinski and R. Palin, *Ind. Eng. Chem.* **51**, 527 (1959).
- 46) R. d'Agostino, G. Ferraro, V. Colaprico, F. Cramarossa and E. Molinari, *3rd Int. Symp. on Plasma Chem.*, IUPAC, vol II G.5.13. Limoges (1977).